

International  
Progress Report

**IPR-05-24**

# Äspö Hard Rock Laboratory

## Äspö Pillar Stability Experiment

### Detailed geological mapping of the pillar blocks

Heta Lampinen  
Posiva

January 2006

***Svensk Kärnbränslehantering AB***

Swedish Nuclear Fuel  
and Waste Management Co  
Box 5864  
SE-102 40 Stockholm Sweden  
Tel 08-459 84 00  
+46 8 459 84 00  
Fax 08-661 57 19  
+46 8 661 57 19



**Äspö Hard Rock  
Laboratory**



Report no.	No.
<b>IPR-05-24</b>	<b>F68K</b>
Author	Date
<b>Heta Lampinen</b>	<b>2006-01-31</b>
Checked by	Date
<b>Carljohan Hardenby</b>	<b>2006-05-30</b>
<b>Christer Andersson</b>	<b>2006-06-12</b>
Approved	Date
<b>Anders Sjöland</b>	<b>2006-06-13</b>

# Äspö Hard Rock Laboratory

## Äspö Pillar Stability Experiment

### Detailed geological mapping of the pillar blocks

Heta Lampinen  
Posiva

January 2006

**Keywords:** Oxidation, Alteration, Spalling, Micro fracturing, Acoustic emission, APSE, TASQ, Thin section, Grain size

This report concerns a study which was conducted for SKB. The conclusions and viewpoints presented in the report are those of the author(s) and do not necessarily coincide with those of the client.



## Abstract

The Äspö Pillar Stability Experiment, APSE, has been performed at Äspö HRL. A pillar was created between two large boreholes ( $\varnothing$  1.75 m) excavated close to each other. In the end of the field work the pillar was sawn into 5 blocks which were removed and it is these that have been mapped.

The dominating rock type in the pillar is Äspö diorite with varying grades of oxidation. The geological mapping was done in decimetre scale, merely by estimating the geological features (i.e. grain size, alteration, oxidation, mineralogy and the structures within the blocks with naked eye and with the help of magnifying glass). According to their appearance the walls of the blocks were divided into smaller units, sub-units that had similar geological features.

For more profound information, a few thin sections of the different oxidation stages of the Äspö Diorite were needed. The rock samples for thin sections were taken from the pillar wall of the deposition hole DQ0063G01, where the major part of the spalling during the pillar stability experiment took place. Features that were studied in the thin sections were; mineralogy, alteration, grain size and the possible microscopic fracturing of the minerals due to spalling.

Alteration - the replacement of plagioclase by quartz and calcite - was found to be as prominent in thin sections as the red oxidation on the rock surface observed with naked eye.



# Sammanfattning

Äspö Pillar Stability Experiment, APSE, har genomförts vid Äspö HRL. En pelare skapades mellan två stora vertikala borrhål ( $\varnothing$  1,75 m) som borrades nära varandra. Fältarbetet avslutades med att pelaren sågades upp i 5 olika block som transporterades bort från experimentområdet. Det är karteringen av dessa block som presenteras i denna rapport.

Den dominerade bergarten i pelaren är Äspödiorit som uppvisar olika grader av oxidering. Karteringen genomfördes i decimeterskala genom att bedöma geologiska egenskaper som kornstorlek, omvandling, oxidation, mineralogi och de strukturer i blocken som kunde upptäckas med ett öga beväpnat med ett förstoringsglas. Vid karteringen delades blocken upp i delenheter där varje delenheter hade liknande egenskaper.

Ytterligare information hämtades in genom att några tunnslip gjordes på Äspödiorit i olika oxidationsstadier. Proverna togs från pelarväggen i deponeringshål DQ0063G01 vilket är den del av pelaren där huvuddelen av spjälkningen ägde rum. Vid mikroskoperingen av tunnslipen studerades mineralogi, omvandling, kornstorlek och möjlig mikrosprickbildning som initierats i samband med spjälkbrotten i pelaren.

Omvandling – utbyte av plagioklas mot kvarts och kalcit – fanns vara lika omfattande i tunnslipen som i de av oxidation rödaktiga områdena av bergytan.





# Contents

<b>1</b>	<b>Introduction</b>	<b>9</b>
<b>2</b>	<b>Project background</b>	<b>11</b>
2.1	APSE	12
2.2	Geological setting	12
<b>3</b>	<b>Detailed geological mapping</b>	<b>15</b>
3.1	Mapping procedures	15
3.2	The sub-units of the Äspö diorite	15
3.2.1	Unaltered Äspö diorite	16
3.2.2	Oxidated Äspö diorite	16
3.2.3	Transitional Äspö diorite	16
3.2.4	Mylonitic Äspö diorite	16
3.2.5	Cataclastic Äspö diorite	16
3.2.6	Epidote (+calcite+chlorite±quartz) veins	17
3.2.7	Mafic inclusions	17
3.2.8	Planes of concentrated K-feldspar crystals	17
3.2.9	Pegmatite veins	18
3.2.10	Calcite (+quartz)-filled tensional fractures	18
3.3	Mapping and photographs of pillar walls	19
<b>4</b>	<b>Thin sections</b>	<b>25</b>
4.1	Sampling	25
4.2	Microscoping results	27
4.2.1	Alteration	27
4.2.2	Grain size	31
4.2.3	Micro fracturing	32
4.2.4	Structural curiosities	32
<b>5</b>	<b>Conclusions</b>	<b>33</b>
<b>6</b>	<b>Summary of the working hypothesis 1-4 in the order as they were presented</b>	<b>35</b>
	<b>References</b>	<b>37</b>
	<b>Appendices</b>	<b>39</b>
	<b>Appendix 1: Thin section descriptions</b>	<b>39</b>
	<b>Appendix 2: Microscope images</b>	<b>43</b>
	<b>Appendix 3</b>	<b>54</b>



# 1 Introduction

The Äspö Pillar Stability Experiment, APSE, is a rock mechanics experiment performed at the Äspö Hard Rock Laboratory. The pillar that was created between two deposition sized boreholes at the 450 m level at the HRL. When the field part of the experiment is analyzed an important part of the background information is the detailed geology of the pillar. To be able to study the geology in quite detail the pillar was sawn into five different blocks which has been thoroughly mapped. The objective for the detailed mapping of the geological features in the APSE blocks was to obtain data that would able correlate with geological properties of the rock (e.g. grain size differences, changes in alteration degree). Clustering of the acoustic emission events during the development of the notch is also possible to correlate with the mapping. In this work, background data was used at some extent during the mapping, but the mapping (e.g. classification of rock units etc.) was not strictly tied to any previous mapping or other experiment data.

Particular interest in this mapping project was put on the open hole wall of the blocks, since it was the location where the notch development occurred.



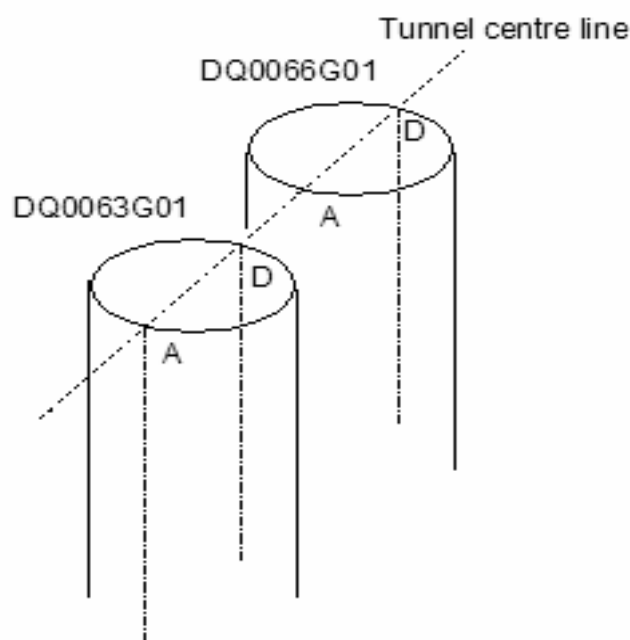
## 2 Project background

The so-known APSE blocks were situated during this mapping project on the elevator shaft hall at the level –340 m in the Äspö HRL (Hard Rock Laboratory). Originally these blocks were sawed from the TASQ tunnel, which is situated at the depth of 450 in the Äspö HRL. The TASQ tunnel itself, and the deposition holes in the tunnel, has been mapped by geologists Björn Magnor and Carljohan Hardenby before this project. That mapping was following the SKB/Äspö standard mapping procedure, where the minimum width of the rock type unit was set to 10 cm. Thinner units were presented as fractures with "rock type filling". Also the APSE blocks were mapped that time in detail, but the emphasis was more on mapping the general features (rock type, fractures) of the blocks, not on the problematic behind spalling.

The data from the previous mapping was used as a reference material in this project and the mapping results, as well as descriptions of all rock types in the TASQ tunnel can be found in Magnor (2004). The detailed fracture maps that are mapped and digitised by Carljohan Hardenby, can be found in the appendix 3 (figures 1-9).

There also exists some amount of background data of the mechanical properties of the rock types in TASQ tunnel (Staub et al. 2004). This information was used at some extent during the mapping, but the mapping (e. g. classification of rock units etc.) was not strictly tied into any previous results or data presented.

In general APSE blocks represent the volume between the two deposition holes, DQ0063G01 and DQ0066G01 (fig. 1), located about one meter apart from each other. They have undergone several rock mechanical test phases of the APSE project before the detailed geological mapping and the blocks have suffered some damage during different stages of transportation. Therefore, the origin of some structures, fractures in particular, in the blocks is questionable.



**Figure 1.** The disposal holes DQ0063G01 and DQ0066G01 in the TASQ tunnel at -450 meters. The APSE pillar is the space between the holes.

## 2.1 APSE

In short, the APSE project is a full-scale rock mechanical experiment with purpose to show the possibilities to predict *spalling* in the fractured rock mass surrounding the canister hole. In this case, the forming and brake-off of thin rock chips from the open hole side of a block wall (represented by a segment of cylinder shaped hole) is called spalling. The area where the spalling was concentrated and where now exists an empty space, is called *notch* (fig. 10). In the APSE experiment the rock surrounding the deposition holes, one with confined pressure and one as an open hole, was heated during a certain timeframe. Heating caused mechanical changes, microscopic fracturing, in the rock of the pillar (e.g. in the five blocks) that were surveyed and recorded as acoustic emission events. In this report the microscopic fracturing is called *micro fracturing*. The 3D location, strength and the timing of each event are known and therefore those can later be compared with the detail mapping of the blocks.

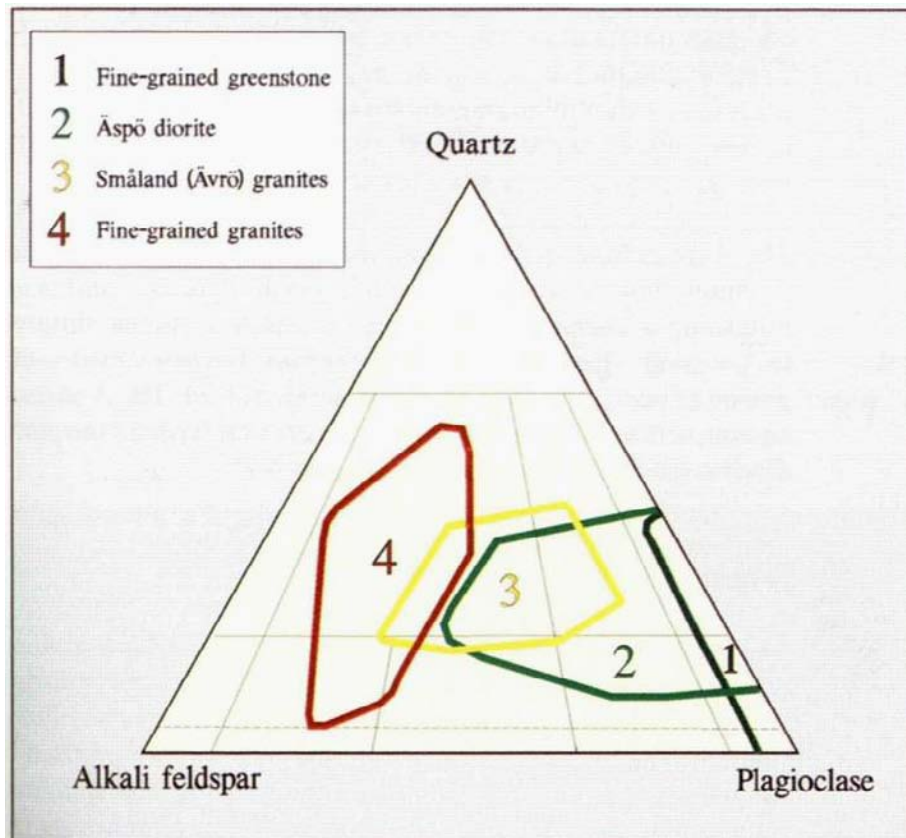
More detailed information of the APSE project can be found in Andersson & Eng (2005).

## 2.2 Geological setting

The TASQ tunnel at the -450 m in Äspö HRL is an area dominated by different varieties of Äspö diorite. The major rock volume consists of unaltered Äspö diorite, but there are also relatively large volumes of oxidized Äspö diorite and sheared, mylonitic Äspö diorite. Also more mafic varieties of Äspö diorite are present. Other rock types are mafic rocks, pegmatite and fine-grained granite. Rock contacts are diffuse, as they are successive transitions from one type of Äspö diorite to another (Magnor 2004).

Usually the Äspö diorite is grey to reddish grey, medium grained, and contain more or less scattered, large crystals of potassium feldspar (K-feldspar). Within the local rock type classification there is a variety of official rock types, such as granodiorites, quartz monzonites, quartz diorites and tonalities. The large number of rock names suggests a rather heterogeneous group, but a look at the modal classification diagram reveals that the group Äspö diorite falls into rather restricted area (fig. 2) (Rhén et al. 1997).

The age of the typical Äspö diorite is dated and the analysis gave a well defined age of  $1804 \pm 3$  million years, which corresponds the crystallisation age of the rock (Rhén et al. 1997).



**Figure 2.** Modal classification of the four main rock groups from the Äspö area, according to IUGS 1973, 1980.

According to Magnor (2004) regional metamorphism appears to be absent or of very low grade. In a few places diffuse foliation can be seen in the Äspö diorite that could be associated with the regional foliation pattern, but it is not accompanied by any visually detectable mineral alteration. Also the hydrothermal alteration is of low grade, and only mapped in association with the TASQ mylonitic shear zone.

The mylonitic Äspö diorite in figure 5 is a constituent of the shear zone, which also intersects the upper volume of the APSE blocks 1 and 2. This zone is classified as brittle-ductile and it has been mapped along the major part of the tunnel, as striking approximately in the same direction as the tunnel,  $N034^{\circ}E$ , and dipping southeast. The shear zone is a dominant structural feature in the tunnel. It is mainly sealed and therefore is considered critical for rock stability (Magnor 2004).





### 3 Detailed geological mapping

The detailed geological mapping was required for specific reason - to be comparable with the development of the spalling which was visually observed and also indicated by the acoustic emission system. Since there are no corresponding previous studies that could be used as a guideline, it was considered important to make some criteria for the mapping. This criteria is presented below as a set of hypothesis that were made in the beginning of the mapping and to which all mapping observations are related. These hypothesis were:

1. The grain size and the differences in the grain size distribution might affect the acoustic emission. For instance, the mafic units that have a small grain size are stiffer than the surrounding rock material.
2. Hydrothermal alteration, which is visible as an oxidation, causes fragility in the rock.
3. Mylonitized zones of some cataclastic parts are less “stable” and therefore the acoustic emission might focus on those. Mylonitized parts also have smaller grain size in relation to other pillar parts.
4. Pre-existing fractures could host acoustic emission clustering if movements along the fracture planes occurred.

#### 3.1 Mapping procedures

The dimensions of the blocks that were mapped were roughly 100 cm of height, 100 cm of width and 120 cm on the B-wall (right side when facing the tunnel front) and correspondingly 150 on the A-wall (left). Observations were done from each side that was visible, excluding only the bottom of each block and the sides of block 5 facing the hole walls. The geological mapping itself was done in decimetre scale, merely by estimating the geological features (eg. grain size, alteration, oxidation, mineralogy and structures) within the blocks with naked eye and with the help of magnifying glass. According to their grain size and alteration the walls of the blocks were divided into smaller units of similar geological feature.

#### 3.2 The sub-units of the Äspö diorite

The pillar blocks consist of a Äspö diorite rock type, which is locally oxidized and sheared with varying degree and with gradual contacts from unaltered up to mylonitized rock. In order to obtain some level of clarity about the rock properties in the different parts of the pillar, the Äspö diorite was divided into the sub-units that are described below and shown in figure 5. One can compare the sub-unit division to photographs of the pillar blocks in the figures 6-9.

### **3.2.1 Unaltered Äspö diorite**

Unaltered diorite is dark bluish grey in colour. Large orange/pink porphyroclasts are slightly flattened and elongated according to the foliation of the rock, and are easily seen from the dark blue rock surface. The diameter of the K-feldspar porphyroclasts varies between 1 and 2 cm.

### **3.2.2 Oxidated Äspö diorite**

In general all rock that is strongly red coloured, which gives an impression that the red mineral, K-feldspar, is more frequent in the oxidated diorite. This might be an illusion, which is simply due to the oxidation itself. Oxidation causes the hematite accessory particles in the crystal lattice scale to turn into red, which eventually leads into the fact that all light coloured minerals (quartz, plagioclase) turn into red. Red is more easily detected in the rock than, for example transparent quartz, and so the amount of K-feldspars seems larger.

### **3.2.3 Transitional Äspö diorite**

In general there is a gradational change between oxidated and unaltered diorite. This change can happen within 5 cm or it might be unclear for tens of centimetres, therefore in some occasions it was found convenient to use term “transitional”. Transitional diorite is redder than unaltered diorite.

### **3.2.4 Mylonitic Äspö diorite**

Mylonitic Äspö diorite is generally planar zones that usually have widths up to 10 or 20 cm. The grain texture is massive-like compared to the surrounding rock. Braided epidote veins are typical within this zone, particularly in the mylonite zone centre. Mylonitic zones are heavily oxidized. In the mylonite there are no large K-feldspar porphyroclasts. Mylonite-stage alteration can be seen in the figure 11.

### **3.2.5 Cataclastic Äspö diorite**

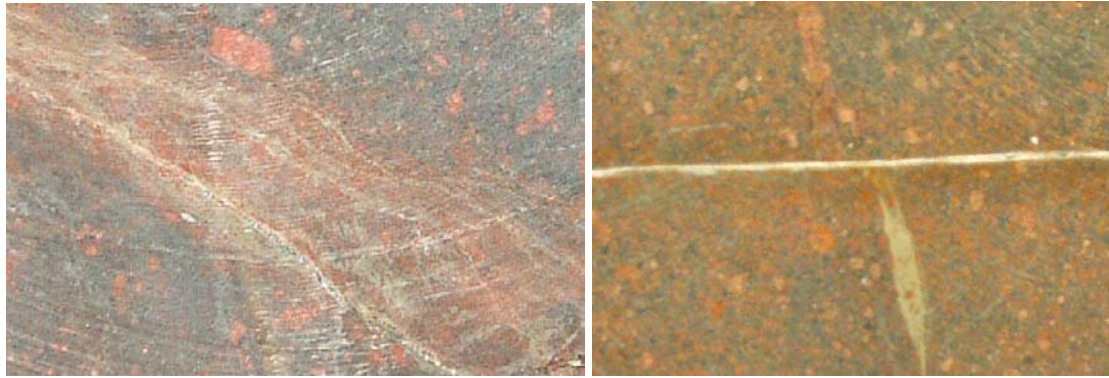
Cataclastic Äspö diorite is observed as lenses of larger, brecciated, diorite, usually in the mylonite zone core. The grain size varies from 0.5 to 2 cm. Cataclastic cores have, in some parts, pegmatite-like appearance. Cataclasts tend to be sharper compared to porphyroclasts in the surrounding rock.

Additional features, for example mineralised veins that could be detected, were taken into notice and recorded into field notes. These were:

### 3.2.6 Epidote (+calcite+chlorite±quartz) veins

1. Irregular, discontinuous and braided system (fig. 3, left) is the most typical epidote vein appearance in the pillar blocks. In the decimetre scale, the epidote filled, semi-ductile-like fractures are planar or slightly undulating and approximately 0.5-3 cm thick. In cm and mm scale the epidote fracture is composed of thin hair-like, braiding epidote veins, which in parts have more matrix- than fracture-like appearance. Epidote colour is yellowish green. These epidote filled fractures have in some occasions, not often, slickenside surfaces, which usually have indicators of sinistral displacement along the fracture plane.
2. Planar and even epidote filled fractures (fig. 3, right) are more rare and usually horizontal and relatively continuous. This fracture is as a single plane that has a width of 0.6 cm. Epidote colour is pale greyish green.

Both types of epidote filled fractures have a clearly detectable oxidated halo that has a width of 5 to 10 cm.



*Figure 3. Braiding (left) and planar (right) epidote-filled fractures.*

### 3.2.7 Mafic inclusions

Orientated mafic (xenolites) inclusions have a diameter of 3-6 cm. The exact age of these xenolites is unknown, but they must be older than the surrounding Äspö diorite, which is  $1804 \pm 3$  Ma old. The inclusions are usually black green in colour and they have deformed, dissolved contacts. The most usual minerals in the inclusions seem to be chlorite, hornblende and possibly biotite. They were observed almost entirely on the topsides of the blocks, which is why only one mafic inclusion is in the figure 5.

### 3.2.8 Planes of concentrated K-feldspar crystals

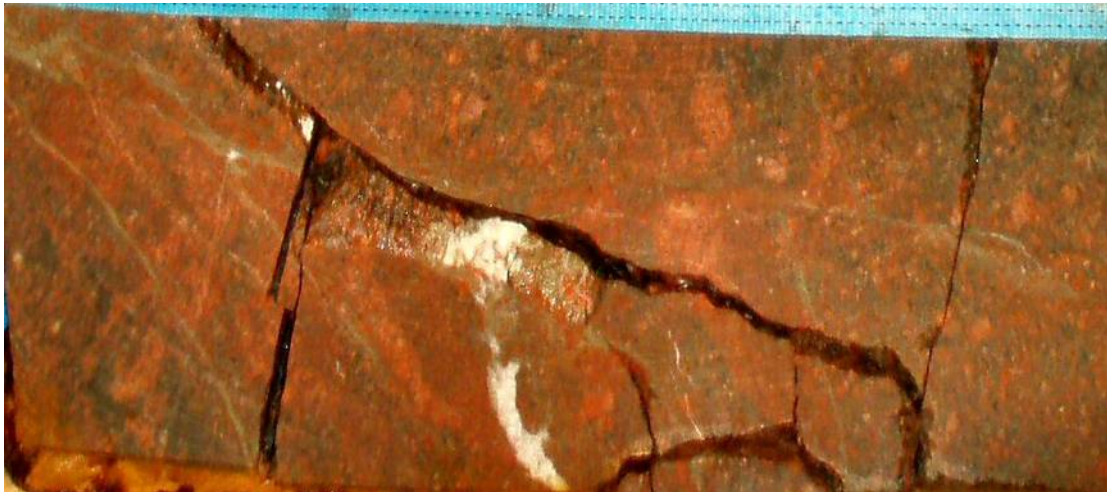
Planes of K-feldspar crystals or some other red mineral are about 0,5-1 cm wide. They don't have vein-like appearance and there doesn't seem to be any fracturing connected to these planes. Planes are elongated with mylonitic structures and most of the epidote-filled fractures, so their formation might relate to the mylonitization.

### 3.2.9 Pegmatite veins

The pegmatite veins are coarse grained, pink and composed mainly of K-feldspar. Pegmatite veins have usually a biotite-rich core. Pegmatite veins are easily detected from the block walls because of their light pinkish orange colour and sharp contacts. Due to their mineralogical composition (feldspars are rigid) they could be one of the most fragile components in the block area.

### 3.2.10 Calcite (+quartz)-filled tensional fractures

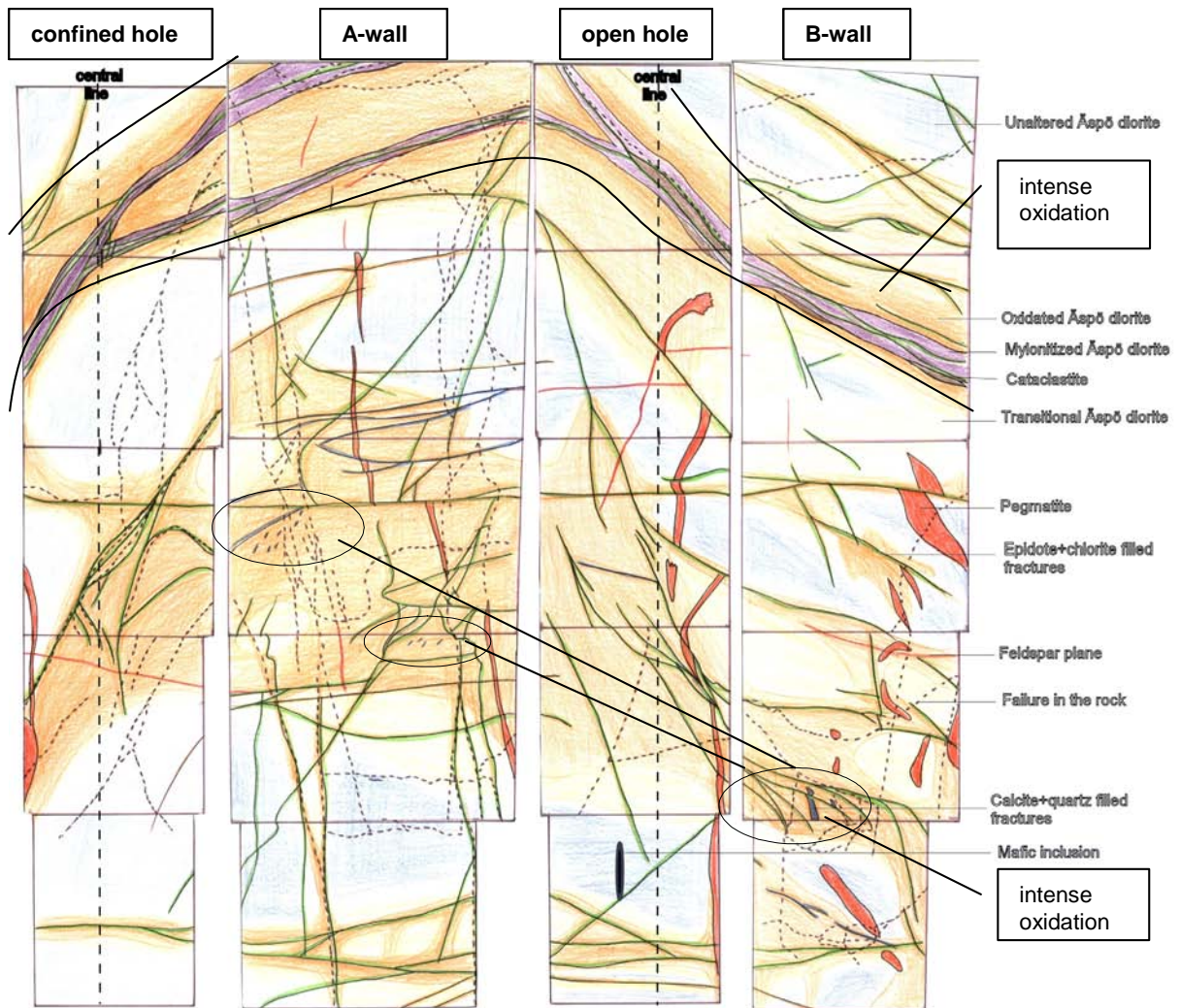
Tensional fractures, filled with calcite and quartz, tend to form in the most competent rock type in the area in question and in the most rigid parts of any given rock (fig. 4). The quantity of calcite in the fractures might be simply due to intensive alteration, which has produced surplus calcite that has filled any possible spaces. The rock surrounding calcite veins is usually strongly oxidized and there are usually several induced fractures in it. This could mean that the rock is relatively more fragile in the intensively altered areas (indicated by "left-over" calcite filled fractures) than in some other parts.



*Figure 4. White calcite filling in a fracture in an intensively oxidated diorite at the bottom part of block 4. The alteration might have lessen the rock strength in these areas.*

In the sketch (fig. 5), walls of the pillar are described side by side. The spalling, of which we are most curious about, took place in the open hole wall. The thick, vertical, dashed lines mark the centreline of the pillar and irregular dashed lines represent induced fracturing.



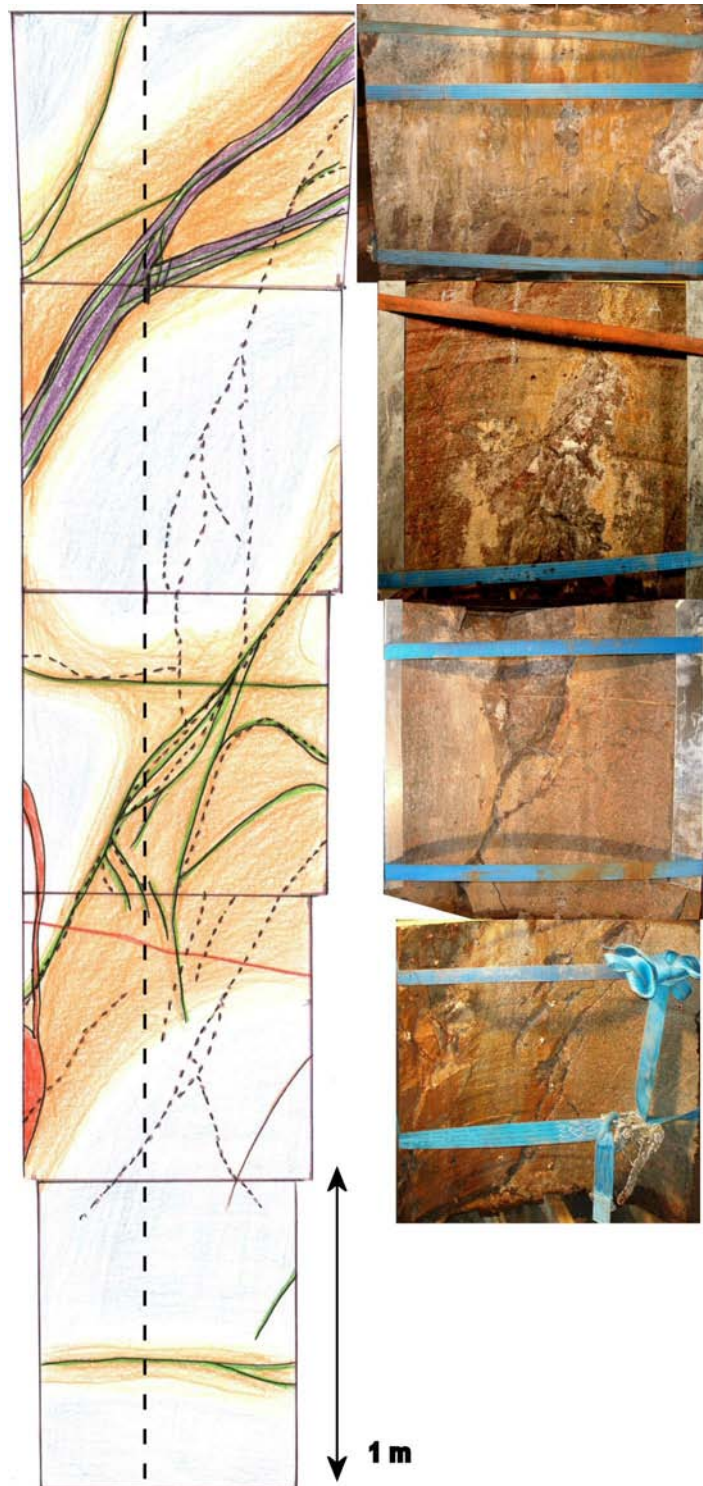


**Figure 5.** All walls of the APSE blocks and the explanations for the colours used in the geological mapping. The dashed lines “Failure in the rock” were induced during the retrieval process of the blocks and are hence neither pre-existing or induced during the heating of the experiment.

### 3.3 Mapping and photographs of pillar walls

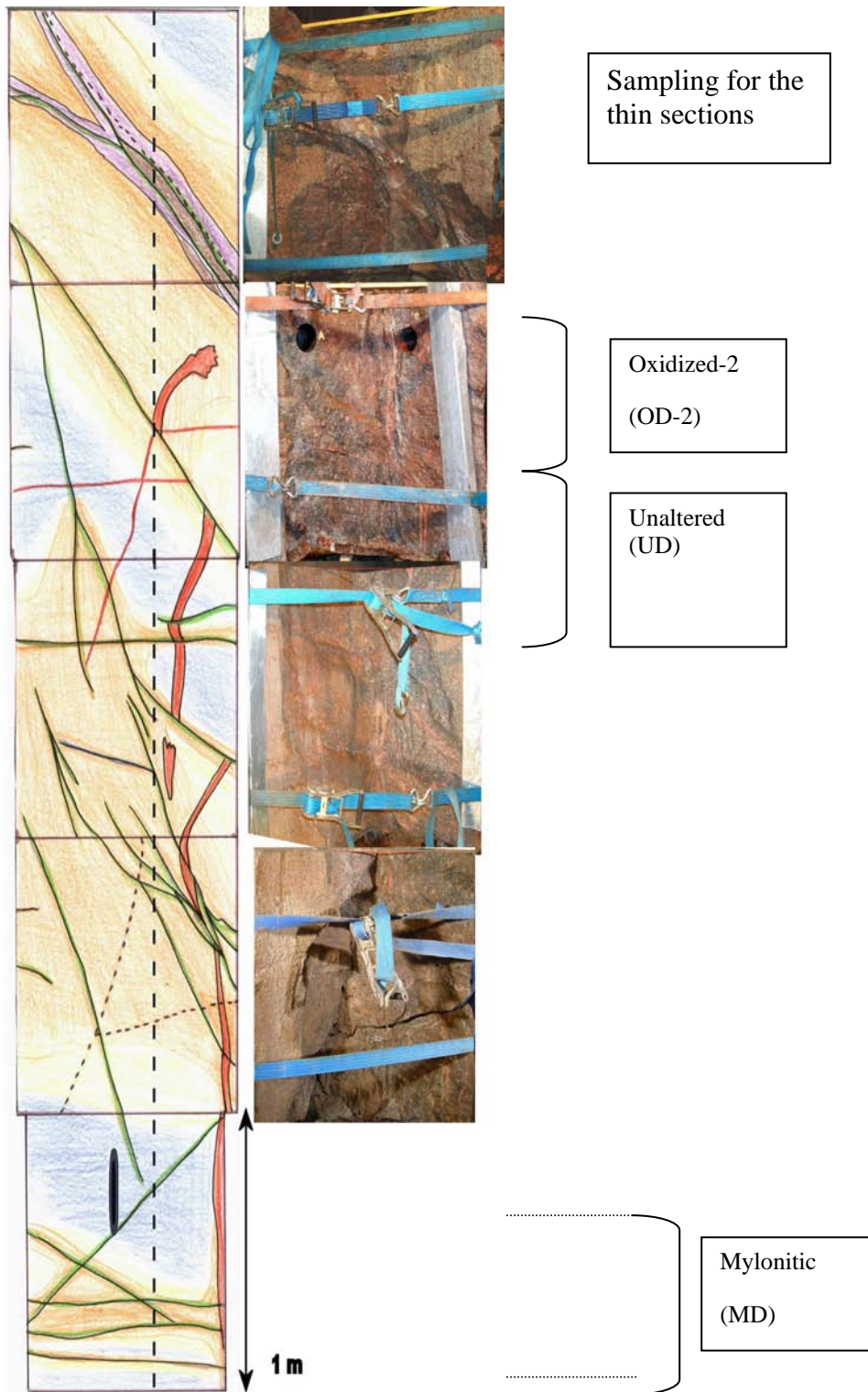
As the block sides were mapped, they were also photographed. Perspective correction was done to the block wall photos in order to get images with right dimensions so that they could be used also in the planned 3D model of the pillar. The interpreted division of the sub-units on the block walls versus photographs of the walls is shown in the figures 6-9, where the mapping is presented to the left and the real image of the rock to the right.

Rock samples for thin sections were selected from rock slabs that were disconnected from the borehole wall due to the spalling during the heating of the pillar stability experiment (see chapter 4). The rock slabs were sampled in depth intervals of 0.5 m. Each interval is stored in separate boxes. The depth (box) interval from which the samples are taken, is marked in figure 7. The thin section sample ID:s are marked on the right in the figure.

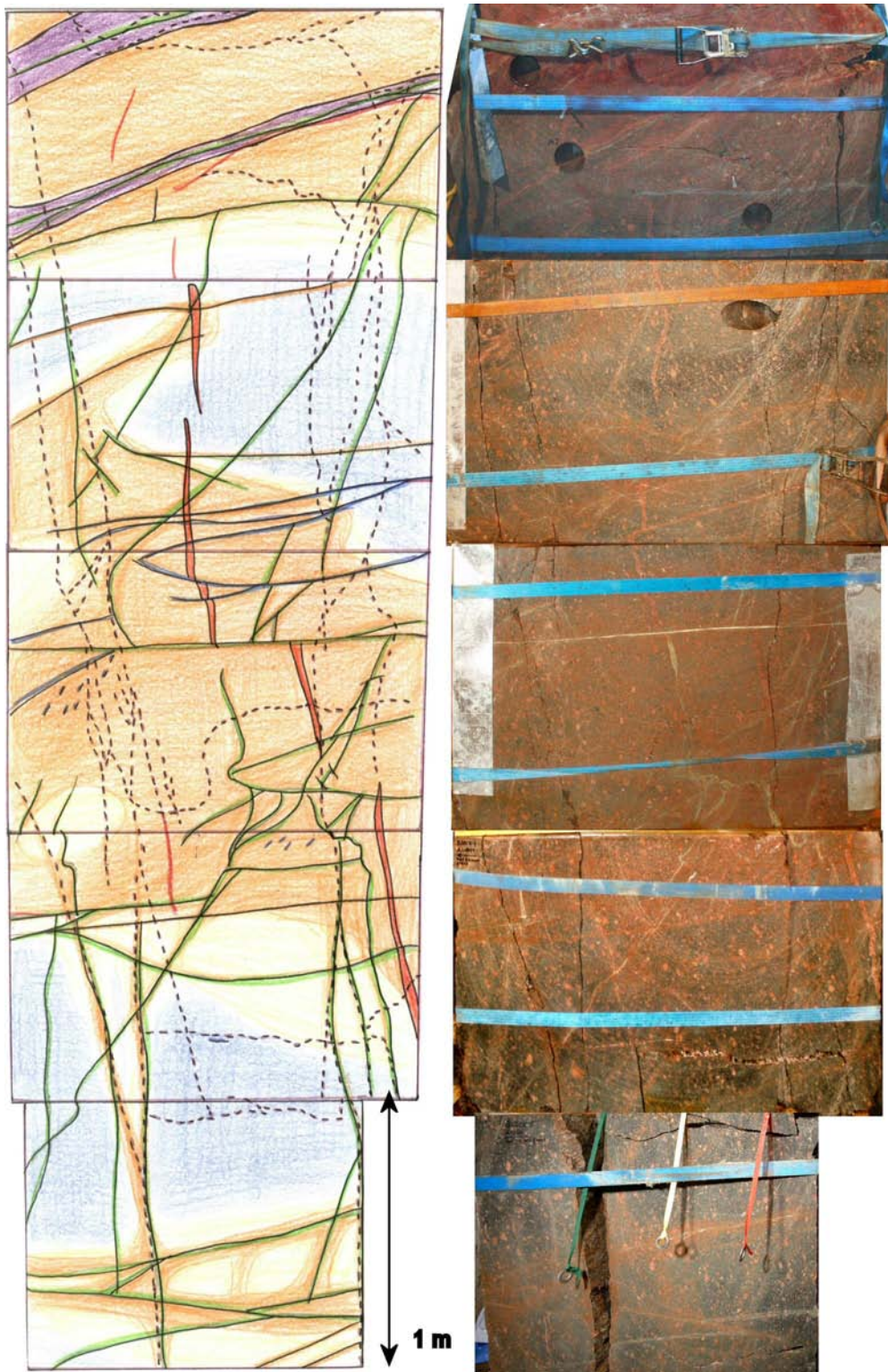


**Figure 6.** Confined (DQ0066G01)hole side of the blocks 1-5; the interpreted geological mapping and photographs. The dashed line in the figure represents the centreline of the pillar/deposition holes (see fig. 1).



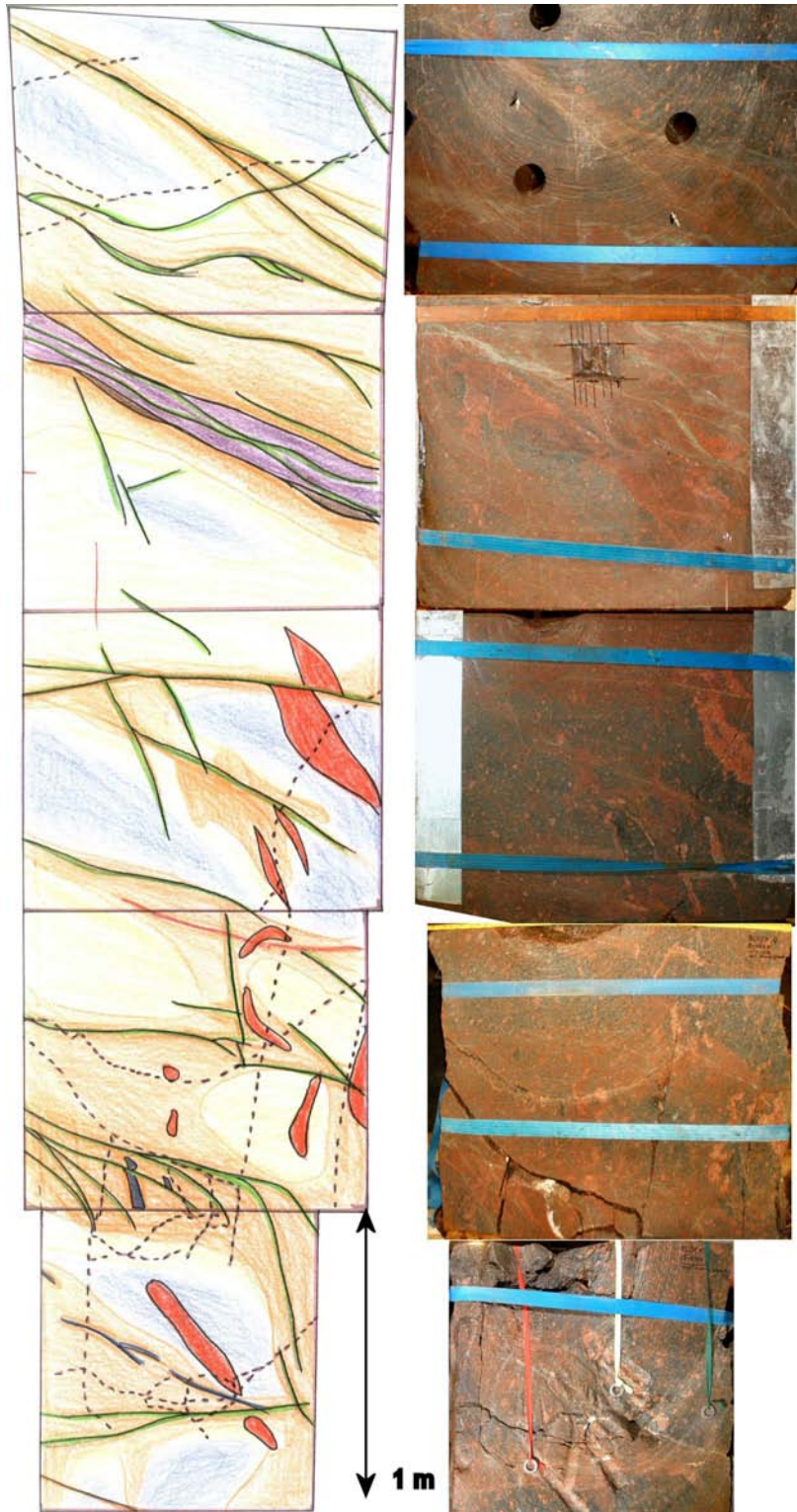


**Figure 7.** The open (DQ0063G01) hole side of the blocks 1-5: the interpreted geological mapping and photos of the block sides and the location of the thin section samples. The dashed line in the figure represents the centreline of the pillar/deposition holes (see fig. 1).



**Figure 8.** The a-wall side(left side when facing the tunnel front) of the blocks 1-5: the interpreted geological mapping and photographs of the same block sides.





**Figure 9.** The b-wall side (right side when facing the tunnel face) of the blocks 1-5: the interpreted geological mapping and photographs of the same block sides.



## 4 Thin sections

For the naked eye, red colouring on the walls of the blocks, gives an impression that the grain size and the quantity of feldspars varies between the oxidized and the unaltered diorite. In general case, the oxidized diorite appears to have a smaller grain size, and more felsic mineralogy. Yet this kind of appearance might be deceiving, so getting some thin sections of the different oxidation stages was found necessary in order to verify the reason behind red colouring.

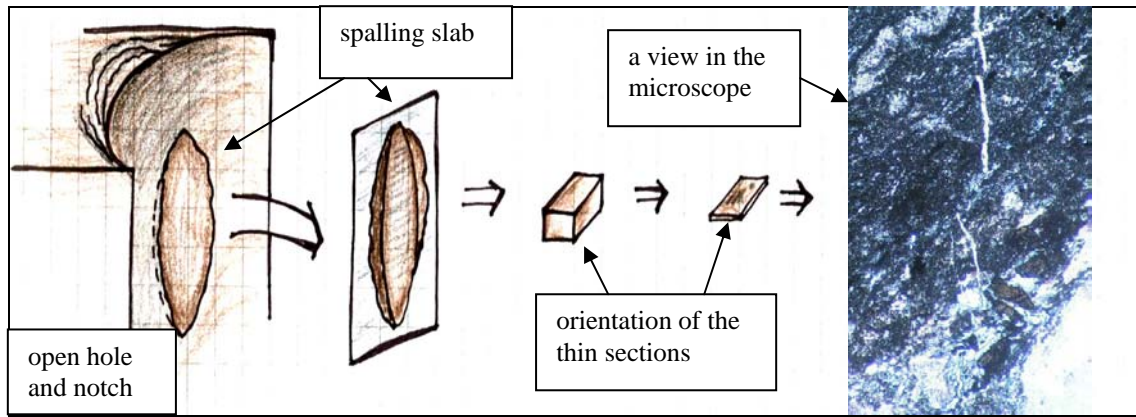
The mineral distribution of the thin sections was quantified with simple point count procedure. In the procedure, the number of identified minerals, on a certain reference line on the thin section, was counted, and from these counts a percentage value for each mineral was established. In the point count measurement 3 horizontal (the longer side of a square) lines with even distances to each other were used.

The rock samples for thin sections were selected from rock slabs that were disconnected from the borehole wall due to the spalling during the pillar stability experiment. The spacing of the original locations of the rock lenses stored in the boxes, of which the thin section specimens were taken, is marked in figure 7. The rock samples from oxidized Äspö diorite and from the mylonitic zone are rock lenses that were disconnected from the borehole (open hole, fig. 6) wall due to the spalling during the pillar stability experiment. In these three thin sections, the section plane is perpendicular to the major orientation of the spalling and therefore micro fracturing of the minerals in these thin sections will also be under investigation (fig. 9).

The four thin sections were manufactured in November 2005 in the rock laboratory of the Geology Department of the University of Turku.

### 4.1 Sampling

As stated above, the rock samples for the thin sections were taken from stored boxes that contained rock slabs produced by spalling (fig. 10). The slabs were collected by Christer Andersson during APSE experiment, and stored in separate boxes that present certain depth intervals in the pillar. Therefore, the exact location of the thin section samples is unknown, although the orientation of the samples OD-1, OD-2 and MD is surely vertical.



**Figure 10.** Orientation of the thin sections in relation to the open hole edge where the spalling took place and the anticipated micro fracturing.

Here also needs to be stated that the sample MD was selected to represent mylonitized diorite purely on the basis of its textural appearance. The sample has all the qualities of a mylonite; extreme oxidation, dense epidote vein network and massive-like grain size. However, the hole depth level, 4,90 m, where the sample is presumably taken, is not mapped as a mylonitic zone. Nevertheless, rock at that depth is extremely oxidized diorite and it in many ways similar to "real" mylonite. The anticipated location of the sample MD is shown in the figure 11.



**Figure 11.** The anticipated location of a sample MD at the depth of 4,90m. Strong oxidation can be seen in the picture.



## 4.2 Microscoping results

Detailed information about the minerals in thin sections, for instance their abundance and relation to each other can be found in the appendix 1. Correspondingly, all taken photos of the microscope images (1-22) are in the appendix 2.

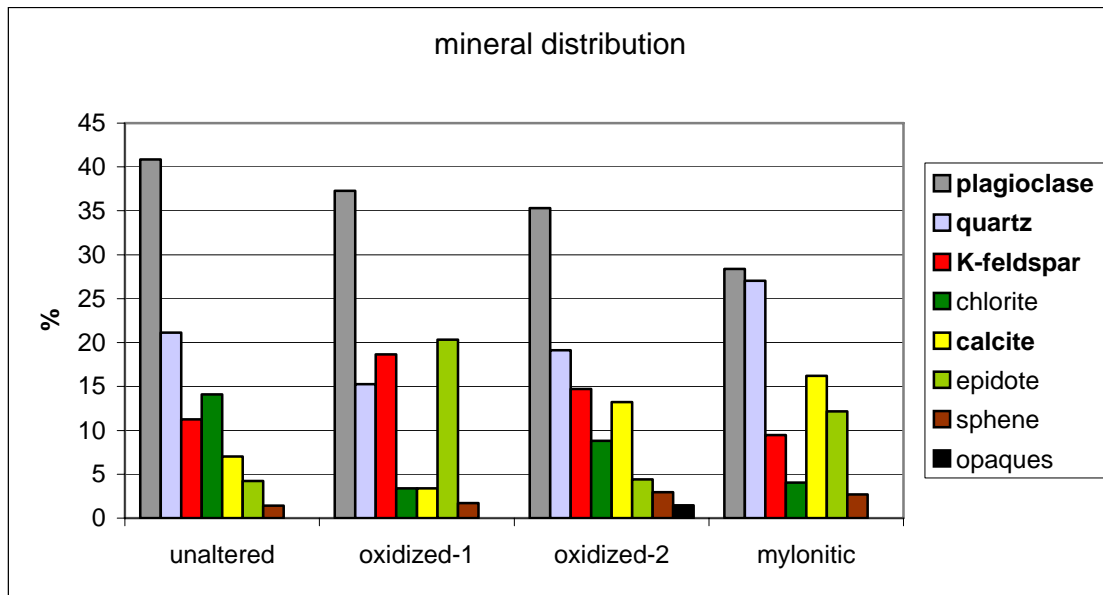
### 4.2.1 Alteration

The general mineralogical distribution of a mean Äspö diorite can be seen in the figure 12. In the figure one can see that plagioclase presents almost a half of the mineralogical composition of the Äspö diorite and the rest is mainly quartz, biotite and K-feldspar.

	Fine-grained greenstone (%)	Äspö diorite (%)	Småland (Ävrö) granite (%)	Fine-grained granite (%)
Quartz	2	15	25	30
K-feldspar	+	12	25	39
Plagioclase	27	46	37	20
Biotite	18	15	7	2
Chlorite	2	1	1	2
Muscovite	-	+	+	3
Fluorite	-	+	+	+
Pyroxene	1	-	-	-
Amphibole	36	2	+	-
Allanite	-	-	+	-
Epidote	9	6	2	2
Monazite	-	-	-	+
Prehnite	+	+	+	+
Pumpellyite	+	+	+	+
Sphene	1	2	1	+
Calcite	+	+	+	+
Apatite	1	1	+	+
Zircon	+	+	+	+
Opaques	2	1	1	1

**Figure 12.** Arithmetic mean values of modal analyses of the four most common rock groups in the Äspö area (Wikman & Kornfält 1995). Äspö diorite is the second on the left.

When this statistics is compared to the chart of mineralogical distribution, in the figure 13, a quite clear difference to the mean mineralogical composition can be seen. Furthermore, the difference to the mean composition correlates with the intensity of oxidation.



**Figure 13.** Distribution of different minerals in the thin sections.

Alteration, the mineral replacement, is as prominent in thin sections as the red oxidation on the rock surface. The total Si content of the rock appears to remain at same level, though the amount of feldspars, plagioclase and K-feldspar lessens, as the amount of quartz and calcite increases (fig. 13). These replacement sequences are presented in the table 1.

**Table 1.** The mineral replacements in the thin sections.

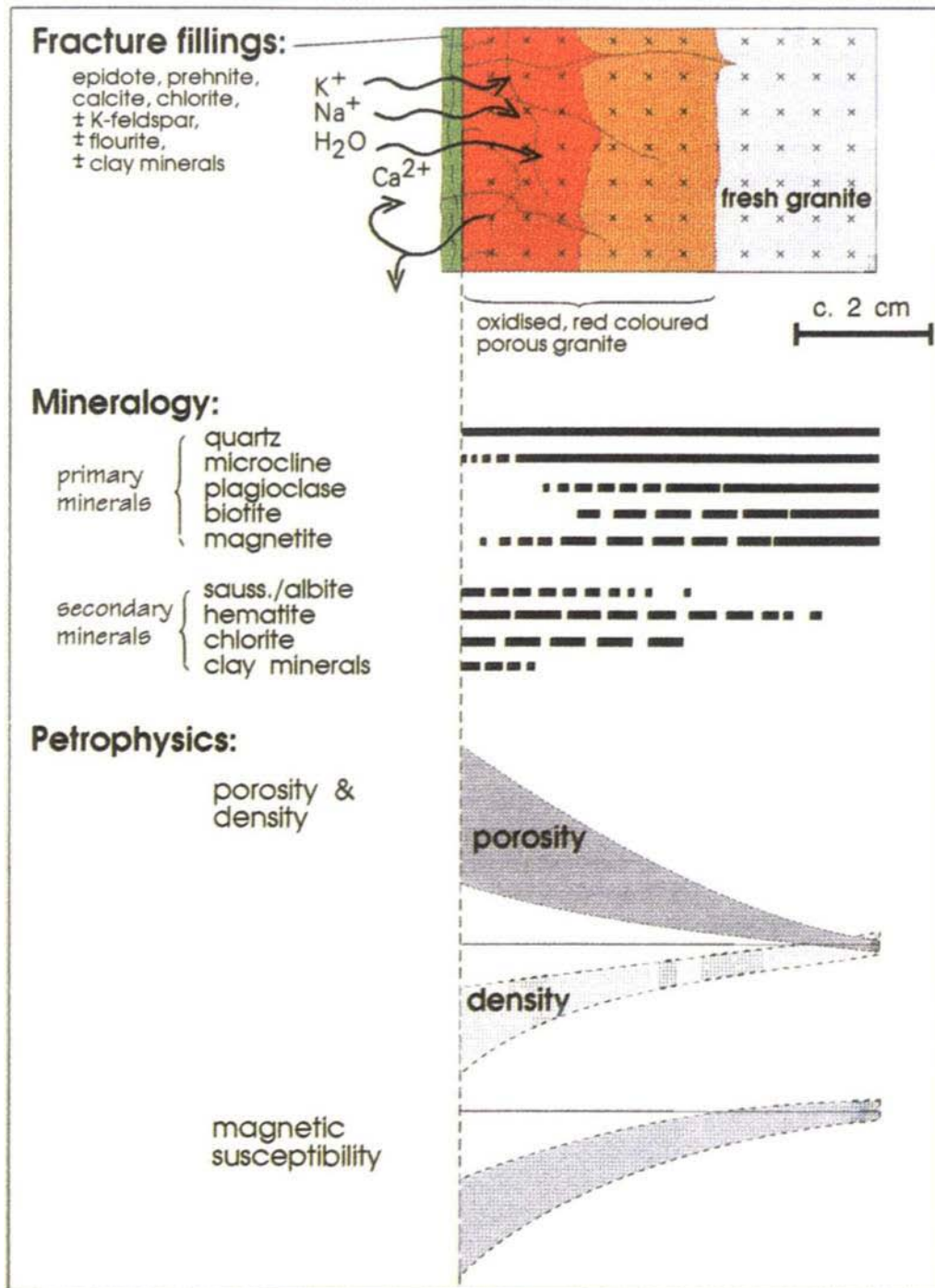
Replacement	Thin section
Plagioclase → quartz + calcite (partial-total)	UD, OD-1, OD-2, MD
K-feldspar → quartz + calcite (partial)	MD
Biotite → chlorite (total)	UD, OD-1, OD-2, MD

It seems that plagioclase has been altered even in the least altered pillar rock sample (microscope images 11, 12, and 14 in the appendix 2). This and the fact that no biotite, which presumably all has altered into chlorite, was found in thin sections, makes one doubt that the alteration is a bit higher than low grade and a bit more disperse than stated in Magnor (2004), at least in the pillar rock volume.

According to the observations, the plagioclase alteration proceeds along a front that moves inward from grain boundaries and fracture and cleavage surfaces. Albite twin planes that can be well observed in the microscope image 13 in the appendix 2, cross the grains without interruption, and the crystal outlines do not change size or shape during alteration. These preserved twinning structures in the plagioclase suggest that the reaction occurs without altering the silicate frame structure of the plagioclase.

In the reaction, the frame structure of feldspars is undisturbed as Ca, Na, and K are exchanged (fig. 14), as the Al and Si become ordered, and as the O is exchanged. The reaction rim most likely shields the reaction front from external fluids (Larson 1997). The reaction rim can be seen in the K-feldspar crystal in the microscope images 17 and 18, in the appendix 2. K-feldspar remains unaltered until the most oxidized parts of the pillar are reached, which makes it probably the most resilient mineral in the Äspö diorite, alongside with the sphene, which is also intact in the thin section of mylonitic rock.

The observed alteration features that were made from the four thin sections are in agreement with the previous study done by Eliasson (1993). In the figure 14 by Eliasson (1993), the alteration features detected in the granitic rocks of Äspö are summarised. It was found that the alteration increased the effective porosity by 2 to 3 times and decreased the density by 0.7 to 1.5 %.



**Figure 14.** Schematic illustration of the most important fractures in the red coloured wall along fractures in the Äspö granitic rock (Eliasson, 1993).

When the microscoping observations are compared to the study of Eliasson (1993), following statements can be made:

1. All thin sections are at least slightly altered. When looked in the mineralogy part of the figure 14, it can be seen that chlorite exists only in the altered parts of the Äspö granitic rocks, and all thin sections in this study contained chlorite.

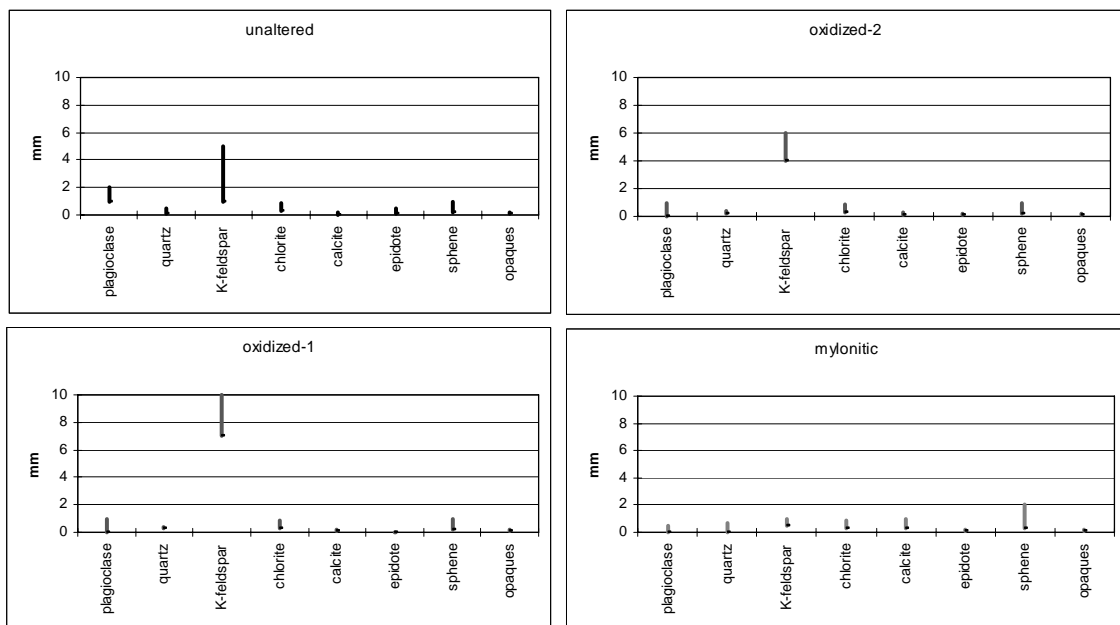


2. The exchange reaction of K, Ca and Na proposed in this text is in agreement with information presented in the figure 14, therefore the alteration process, suggested for the Äspö diorite in this text, is most likely rightly concluded.
3. In figure 14, the porosity of a rock increases as the density of the rock decreases, as the stage of alteration grows. This implies that the strength of the rock is most likely to decrease as these two factors behave in this manner.

As a final statement to the observations and interpretation presented above can be said that, the more the Äspö diorite in the APSE pillar rock volume is oxidized, the more it is altered which might affect the strength properties.

#### 4.2.2 Grain size

The grain size of the minerals does not seem to be affected by the alteration stage of the sample. This can be noted from the mineral grain size charts in the figure 15. The grain size variation in both unaltered and oxidized thin sections is almost similar. The only exception is in the mylonite sample, which lacks large K-feldspar porphyroclast. This change in mineral grain size is most likely related only to mechanical, brittle shearing that has brecciated also to the rock. The brecciated minerals (cataclasts) within the epidote veins can be seen in the microscope images 13, 14, 21 and 22, in the appendix 2.



**Figure 15.** Grain size variation of all minerals in thin sections.

Alteration itself doesn't seem to brake minerals and therefore lessen grain size. Changes in the mineral sizes seem to be purely related to shear structures.

The shear structures with cataclastic, erratically located, mineral crystals might be less stable than other parts of the rock volume.

### 4.2.3 Micro fracturing

The anticipated micro fracturing is observed with some certainty only in one thin section in the microscope images 9 and 10 in the appendix 2. The micro fracture observed this far was in the epidote + chlorite band and was cutting foliation. The orientation, which is parallel to spalling geometry, and the fact that the fracture in the microscope image 10 in the appendix 2, has a coarse trace that doesn't follow crystal boundaries, and is without mineral filling, would suggest that its origin is due to APSE experiment.

For instance the brittle fracturing in the MD sample (microscope images 19 and 20) is smoother and more planar compared to the anticipated spalling related fracturing in the microscope image 10. Micro fracturing does not seem to follow any previous structure in the rock sample and it cross-cuts for example the foliation in the rock.

The brittle fracturing in the MD sample has a smooth trace, which implies that this fracturing is not formed in the spalling process, but during or after the formation of mylonitic shear structures. Fracturing could be due to more fragile quality of a rock that is caused by intensive alteration. On the other hand the relation of alteration and fracturing could be other way a round and intense alteration could be due to fracturing and induced fluid activity due to it.

The fracturing in the UD thin section (microscope images 1 and 2, appendix 2) might also be related to spalling but, since the exact orientation and location of a thin section hand specimen is not known, it cannot be stated as certain.

To learn more about micro fracturing, more studies needs to be done. Since the amount of data about the topic at the moment is miniscule, it is impossible to say anything about the micro fracturing symmetry, nor if it has a tendency to be present in some particular compositional varieties in the rock.

### 4.2.4 Structural curiosities

As a curiosity, photos of the microscope images of the symplectite and perthite structures were taken. These two microstructures are typical for metamorphic granitoid rocks, such as Äspö diorite. These structures relate to metamorphic history of Äspö diorite and have therefore no affect on the question of spalling and its relation to geology.

Symplectite structure was observed in the K-feldspar crystal microscope image 3 in the appendix 2. Symplectites are fine-grained intergrowths of two or more phases and can be found in high-grade metamorphic rocks.

Perthitic lamellae can be found in the K-feldspar crystal in the microscope images 5 and 6 in the appendix 2. Perthite is a structural variety of the potassium feldspars microcline and orthoclase ( $KAlSi_3O_8$ ). Alkali feldspar formed at relatively high temperature (above 660 °C) is a solid solution of potassium (K) and sodium (Na) feldspar. As the system cools the solid solution becomes unstable and the two feldspars separate by exsolution into lamellae of albite (Na) and microcline (K).

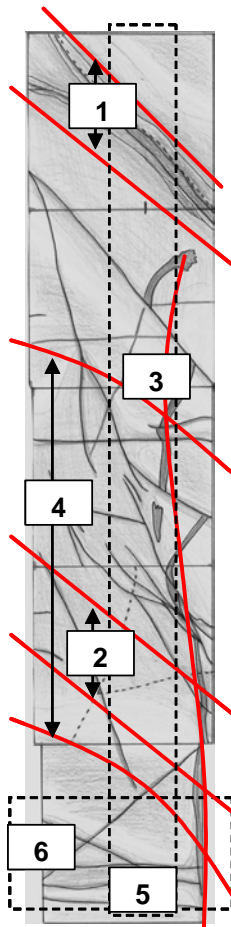
## 5 Conclusions

Alteration. The extent and strength of oxidation, seems to affect on the rock fragility. The more oxidized the rock is, the more rigidly it could be expected to behave. This would mean that the clustering of acoustic emission events could be targeted towards oxidized parts of the rock.

The mylonitic shear zone. It is strongly oxidized and the rock is also brecciated. Therefore, mylonitic shear zone is also a potential target for acoustic emission clustering.

The pegmatite vein. This might also gather some amount of acoustic events due to its felsic composition. The rock types with higher SiO<sub>2</sub> content seem to behave in more rigid fashion in relation to others.

According to this theory, the areas of the pillar rock volume that would be most likely to host acoustic emission events would most likely be somewhat related to geological features (cf. point 4 in the paragraph of working hypothesis). These areas, where the clustering of the acoustic emissions is expected to happen on the open hole side of the pillar according to geological properties, is shown in the figure 16. The number codes in the figure correspond the geological reason for clustering and the red lines and the dashed lines show the area.



1. Mylonitic shear zone and the cataclastic parts within.
2. Strongly oxidized diorite, which is intensively altered and shows signs, such as calcite and quartz filled fractures, of previous rigid behaviour.
3. Pegmatite vein.
4. Oxidized diorite.
5. If the clustering would focus quite evenly close to the pillar central line, it could be interpreted to relate purely on the geometry of the cylinder shaped hole.
6. If the exact location of sample MD can be verified to this depth, here is an area of intense oxidation.

Micro fracturing can evidently be seen in the thin sections. Since the amount of data about the topic is at the moment miniscule, it is impossible to say anything about the micro fracturing symmetry, nor if it has a tendency to be present in some particular compositional varieties in the rock.

**Figure 16.** Expected clustering of acoustic emission events at the open hole side.



## **6 Summary of the working hypothesis 1-4 in the order as they were presented**

1. The affect of grain size variations to spalling seems miniscule, especially, since the amount of mafic rock volume is very small.
2. The hydrothermal alteration seems to be likeliest factor to have an affect on the micro fracturing and spalling.
3. The unstability of the rock in the mylonitic shear structure may have affect on the spalling geometry and the acoustic emission clustering.
4. The affect of pre-existing structures was not investigated to the needed extent in this study to be able to make conclusions.



## References


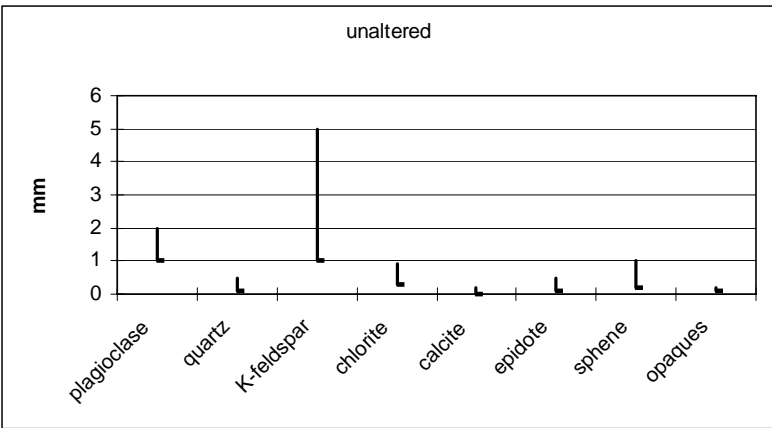
- Andersson J C. and Eng A 2005.** Äspö Pillar Stability Experiment. Final experiment design, Monitored data and observations. SKB report R-05-02.
- Eliasson, T. 1993.** Mineralogy, geochemistry and petrophysics of red-coloured granite adjacent to fractures. SKB TR 93-06, Svensk Kärnbränslehantering AB.
- IUGS SUBCOMMISSION ON THE SYSTEMATICS OF IGNEOUS ROCKS 1973.** Classification and Nomenclature of Plutonic Rocks. Recommendations. N. Jb. Miner. Mh. 1997, H4, 149-164.
- IUGS SUBCOMMISSION ON THE SYSTEMATICS OF IGNEOUS ROCKS 1980.** Classification and Nomenclature of Volcanic Rocks. Lamprophyres, Carbonatites and Melitic Rocks. Geol. Rundschau 69, 194-207.
- Larson, P.B. 1997.** Coupled plagioclase exchange reactions in natural hydrothermal system. Seventh Annual V. M. Goldschmidt Conference.  
<http://www.lpi.usra.edu/meetings/gold/pdf/2181.pdf>
- Magnor, B. 2004.** Äspö Hard Rock Laboratory. Äspö Pillar Stability Experiment. Geological mapping of tunnel TASQ. SKB IPR-04-03, Svensk Kärnbränslehantering AB.
- Staub, I., Andersson, J.C. & Magnor B., 2004.** Äspö Pillar Stability Experiment. Geology and mechanical properties of the rock in TASQ. SKB R-04-01, Svensk Kärnbränslehantering AB.
- Rhén, I. (ed.), Gustafson, G., Stanfors, R. & Wikberg, P. 1997.** ÄSPÖ HRL - Geoscientific evaluation 1997/5. Models based on site characterization 1986-1995. SKB TR 97-06, Svensk Kärnbränslehantering AB.
- Wikman, H. & Kornfält K-A. 1995.** Updating the lithological model of the bedrock of the Äspö area. SKB PR 25-89-06, Svensk Kärnbränslehantering AB.




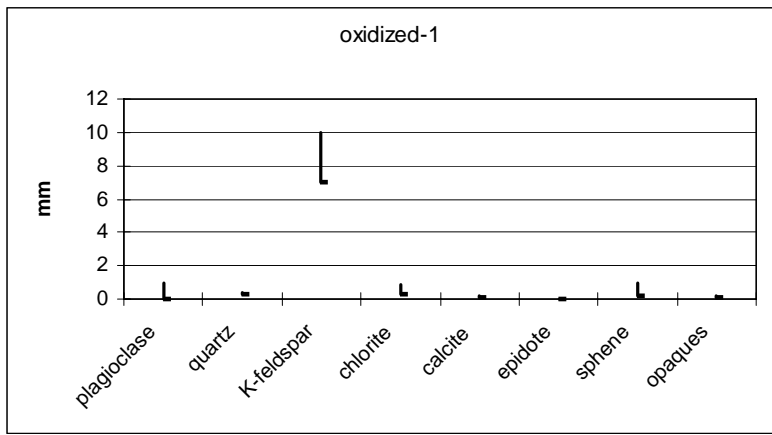


# Appendices


## Appendix 1: Thin section descriptions

<p><b>Sample ID:</b> Unaltered Äspö Diorite (UD)</p>		<p><b>Hand specimen figure:</b></p> 	
<p><b>Location:</b> Sample is from the box 3,30-2,70 (04_10_13, DQ0063)</p>			
<p><b>Microscope images:</b> 1, 2, 3, 4, 5, 6</p>			
<p><b>Description:</b> Slightly foliated and granoblastic. Edges of the K-feldspar porphyroclasts are red-coloured. Quartz, chlorite, calcite and epidote are as a matrix. Plagioclase is moderately replaced by calcite and chlorite. Microscopic fracturing seems to be perpendicular to the foliation.</p>		<p><b>Grain size distribution:</b></p> 	
Mineral	%	Description	
Plagioclase	41	Subhedral, strongly (~20-50 % of the grains) displaced by calcite ( $\pm$ chlorite). Interiors are usually intact and have perthite twinning.	
Quartz	21	Subhedral, usually as porphyroclasts/blasts (smaller grains concentrated into clumps), matrix-like compared to plagioclase.	
Chlorite	14	Anhedral, irregular shapes, usually matrix-like accompanying epidote and quartz, mineral fibres tend to follow foliation.	
K-Feldspar	11	Euhedral, usually as large porphyroclasts that have perthite/micropertite structures, very little alteration or deformation, grains are little rounded and at boundaries of the larger crystals there are K-feldspar-quartz mineral intergrowths (symplectites).	
Calcite	7	Anhedral in general, some subhedral, larger grains, usually as a microscopic dissemination within the plagioclase grains or at the boundaries of the plagioclase and quartz grains.	
Epidote	4	Subhedral, grain boundaries are deformed in a corroded style, some twinning in some crystals.	
Sphene	1	Euhedral, typically diamond-shaped, mainly intact.	
Opaque	---	Euhedral, accessory, probably pyrite.	

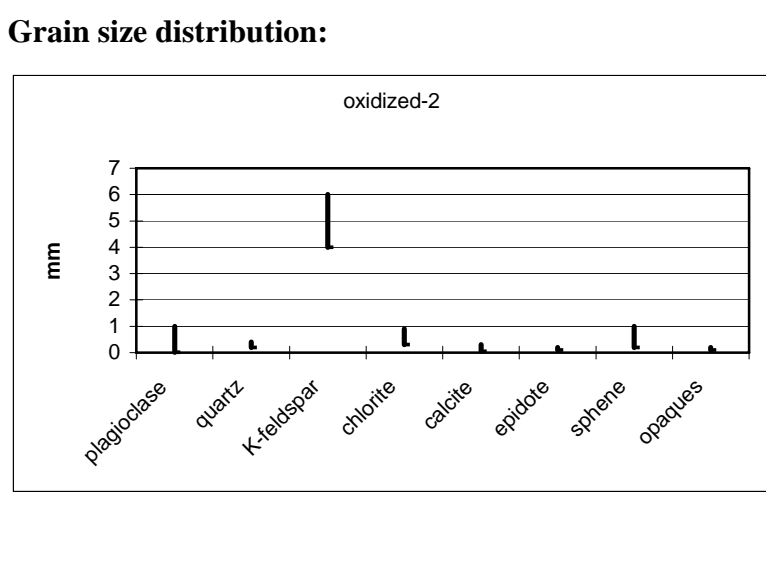
<p><b>Sample ID:</b> Oxidized Äspö Diorite 1 (OD-1)</p>	<p><b>Hand specimen figure:</b></p>
<p><b>Location:</b> Sample is from the box 3,30-2,70 (04_10_13, DQ0063, “+det I botten”).</p>	
<p><b>Microscope images:</b> 7, 8, 9, 10</p>	

<p><b>Description:</b> Two intensively oriented shear bands (mainly chlorite), couple large K-feldspar porphyroclasts (0,7-1,5 cm). All light/transparent minerals seem to have reddish to brownish hue cast over them. Quartz has smaller grain size compared to UD sample, and the grain size seems to be smallest in places the calcite is abundant.</p>	<p><b>Grain size distribution:</b></p> 
-----------------------------------------------------------------------------------------------------------------------------------------------------------------------------------------------------------------------------------------------------------------------------------------------------------------------------------------------------------------	----------------------------------------------------------------------------------------------------------------------------


Mineral	%	Description
Plagioclase	37	Subhedral/anhedral, strongly (~30-60 % of the grains) displaced by calcite ( $\pm$ chlorite). Has very dull reddish/brownish hue on top. Interiors, when intact, and have perthite twinning. In places almost amorphous (glass-like)
Epidote	20	Anhedral, messy-looking mineral that has small, almost undetectable grain size. Dull reddish/brownish hue on top.
K-Feldspar	19	Euhedral, large chrystals that are slightly altered. Edges of the minerals have broken into smaller grains. Some calcite and chlorite inclusions.
Quartz	15	Subhedral, usually as porphyroclasts/blasts (smaller grains concentrated into clumps). Bright mineral compared to feldspars.
Calcite	3	Anhedral/subhedral, usually as a microscopic dissemination in the plagioclase grains or at the boundaries of the plagioclase and quartz grains.
Chlorite	3	Anhedral, irregular shapes, usually matrix-like accompanying epidote and quartz, mineral fibres tend to follow foliation.
Sphene	2	Euhedral, typically diamond-shaped, some grains are rounded.
Opaque	---	Euhedral/subhedral, accessory, probably pyrite

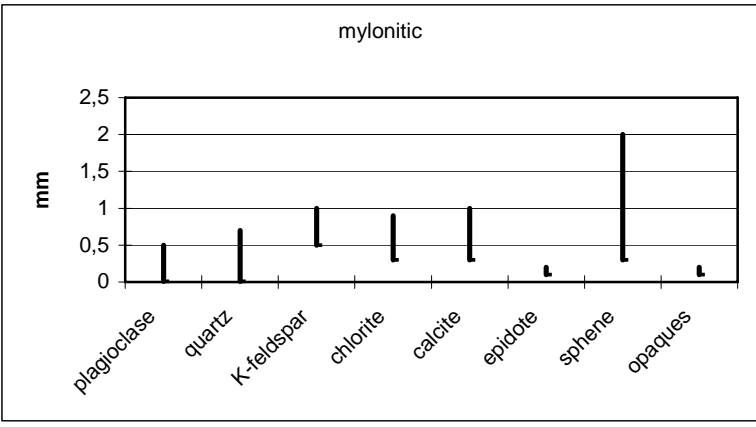
<p><b>Sample ID:</b> Oxidized Äspö Diorite 2 (OD-2)</p>	<p><b>Hand specimen figure:</b></p>
<p><b>Location:</b> Sample is from the box 2,70-2,10 (04_10_14, DQ0063)</p>	
<p><b>Microscope images:</b> 11, 12, 13, 14</p>	

**Description:**  
Quite undisturbed diorite, though in the middle of the section there is one intensively sheared ( $\varnothing$  1 cm) cataclastic band. Matrix in the band has miniscule grain size (plagioclase+calcite+epidote), and the clasts are plagioclase, sphene, K-feldspar and quartz. Chlorite and quartz are in general as a matrix in the rock and are also the most easily distinguishable.



Mineral	%	Description
Plagioclase	35	Subhedral/anhedral, strongly (~30-70 % of the grains) displaced by calcite ( $\pm$ chlorite). Has very dull reddish/brownish hue on top. Interiors, when intact, and have perthite twinning. In places almost amorphous (glass-like)
Quartz	19	Subhedral, usually as porphyroclasts/blasts (smaller grains concentrated into clumps). Bright mineral compared to feldspars.
K-Feldspar	15	Euhedral, large crystals that are slightly altered. Edges of the minerals have broken into smaller grains. Some calcite and chlorite inclusions.
Calcite	13	Anhedral/subhedral, usually as a microscopic dissemination in the plagioclase grains or at the boundaries of the plagioclase and quartz grains. Grain size is in places miniscule.
Chlorite	9	Anhedral, irregular shapes, usually matrix-like accompanying epidote and quartz, mineral fibres tend to follow foliation.
Epidote	4	Anhedral, messy-looking mineral that has small, almost undetectable grain size. Dull reddish/brownish hue on top.
Sphene	3	Euhedral, typically diamond-shaped, some grains are rounded.
Opaque	1	Euhedral, accessory, probably pyrite

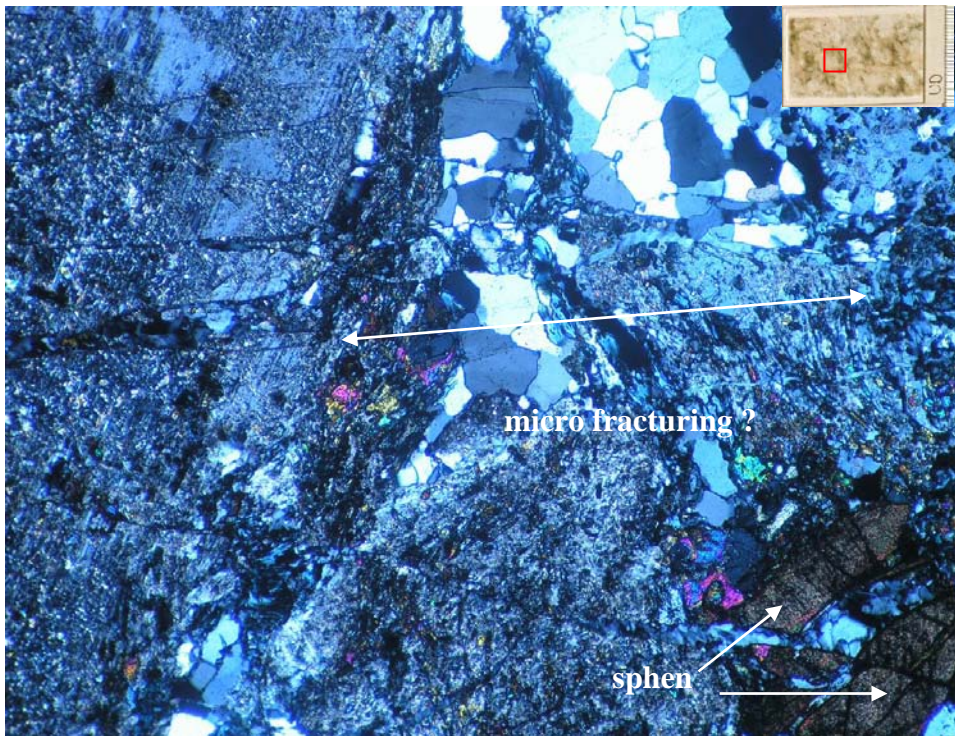
<b>Sample ID:</b> Mylonitic Äspö Diorite (MD)	<b>Hand specimen figure:</b>
<b>Location:</b> Sample is from the box 4,9-4,3 (04_09_28, “+det I botten”)	
<b>Microscope images:</b> 14, 15, 16, 17, 18, 19, 20, 21, 22	

<b>Description:</b> Tight epidote vein network, which has strong reddish/brownish colour hue on top. Epidote veins cut K-feldspar and plagioclase grains. There are no large K-feldspar phenocrysts.	<b>Grain size distribution:</b> 
---------------------------------------------------------------------------------------------------------------------------------------------------------------------------------------------------------	------------------------------------------------------------------------------------------------------------------------

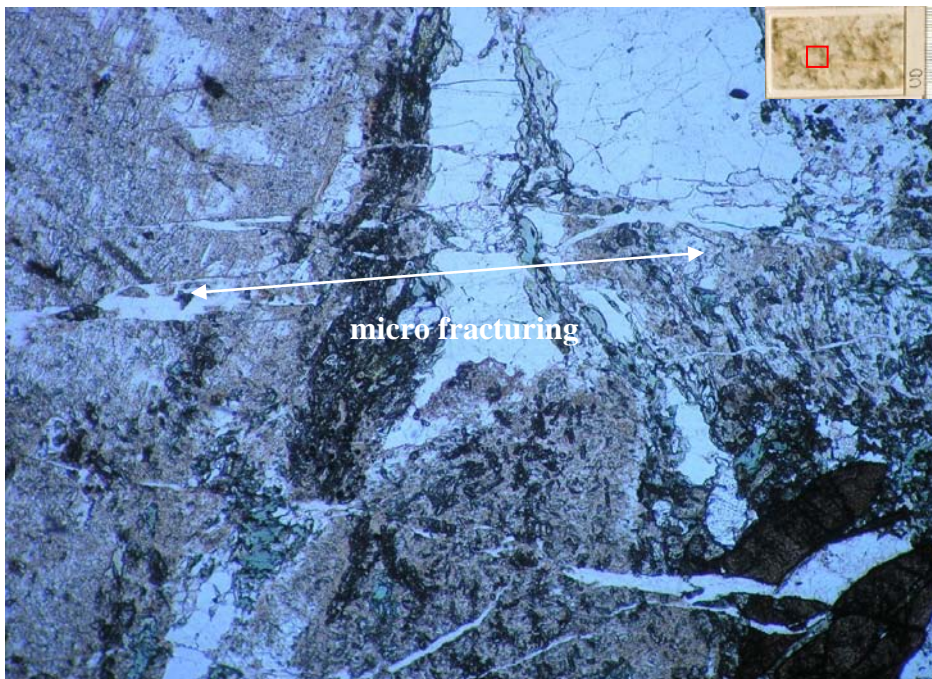
Mineral	%	Description
Plagioclase	28	Subhedral/anhedral, almost totally (~50-85 % of the grains) displaced by calcite and quartz (±chlorite). Has very dull reddish/brownish hue on top. Some remnants of perthite twinning in the interiors of mineral grains.
Quartz	27	Subhedral, usually as porphyroclasts/blasts (smaller grains concentrated into clumps). Bright mineral compared to feldspars.
Chlorite	16	Anhedral, irregular shapes, usually matrix-like accompanying epidote and quartz, mineral fibres tend to follow foliation. Easy to distinguish (not altered).
Calcite	16	Anhedral/subhedral, usually as a microscopic dissemination in the plagioclase grains, or at the boundaries of the plagioclase and quartz grains, in which case mineral grains are up to 1 cm diameter.
Epidote	12	Euhedral/subhedral and bright green (compared to epidote in other thin sections), which implies that it is placed after main alteration-event.
K-Feldspar	4	Euhedral, though the edges of the minerals have been displaced by quartz and calcite, which gives the grains a concentric appearance. No large phenocrysts.
Sphene	3	Euhedral and rather large grain size compared to other thin sections
Opaque	---	Euhedral, accessory, probably pyrite



## Appendix 2: Microscope images

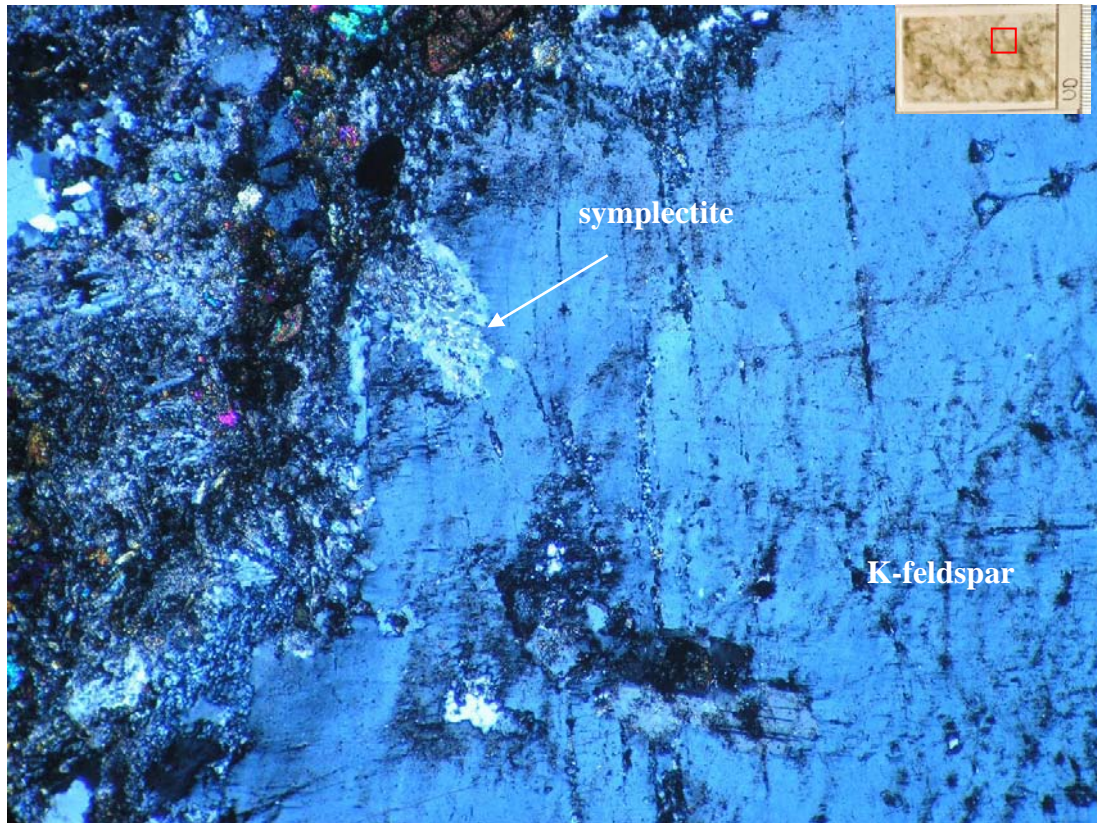


**Microscope image 1:** Unaltered Äspö Diorite (UD) in polarized light. Possible micro fracturing that tends to cut foliation. The connection to the spalling is impossible to verify, since the orientation of the sample is unknown. Nice, euhedral sphene crystals. Width of the image is 4 mm.



**Microscope image 2:** Image 1 in non-polarized light. The horizontal fractures that could be due to APSE project can be easily seen in the image. Width of the image is 4 mm.



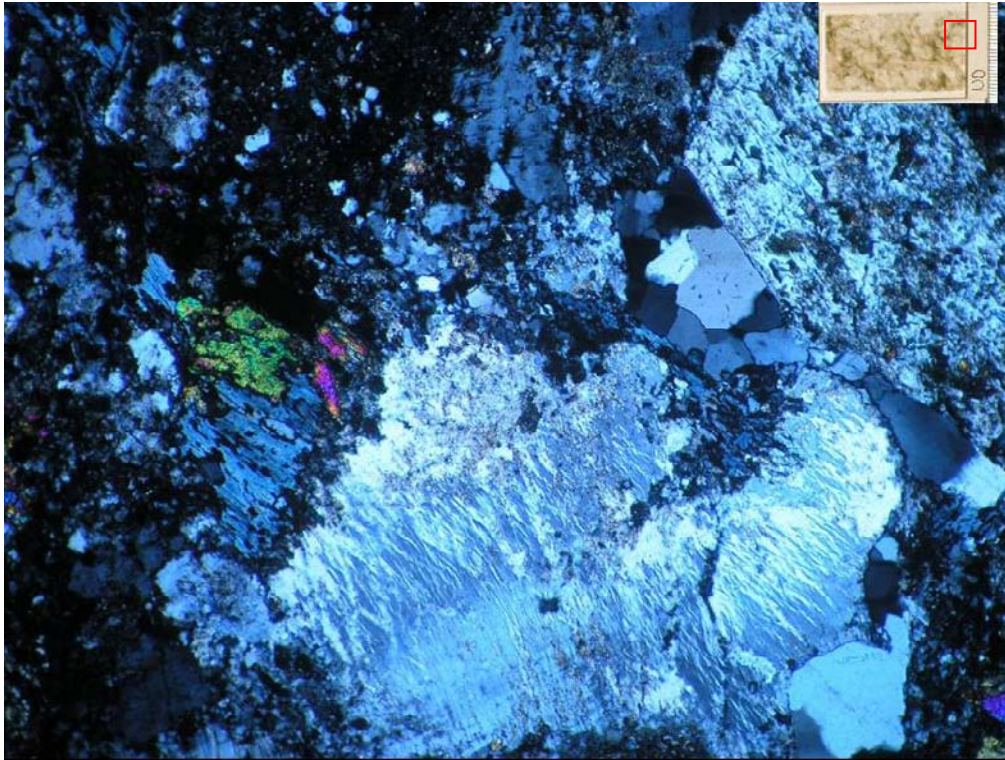


**Microscope image 3:** Unaltered Äspö Diorite (UD) in polarized light. Feldspar-quartz intergrowth structure: symplectite. Note: no alteration at the edge of crystal. Width of the image is 4 mm.

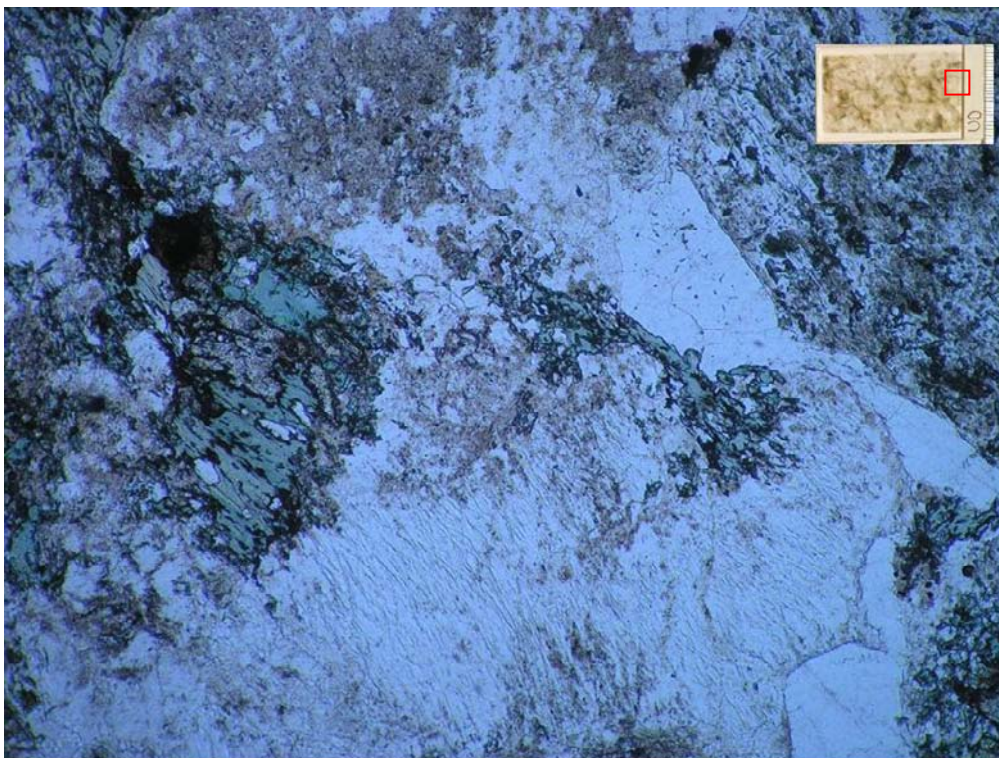


**Microscope image 4:** Image 2 in non-polarized light. Width of the image is 4 mm.



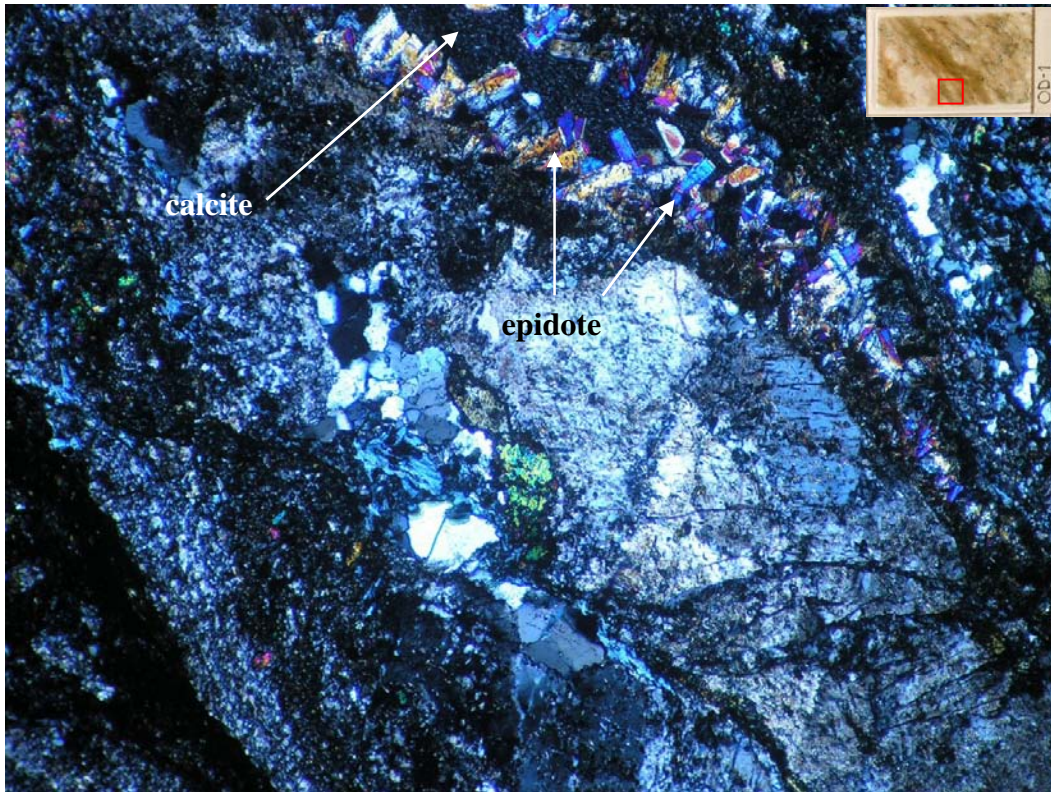


**Microscope image 5:** *Unaltered Äspö Diorite (UD) in polarized light. Feldspar grain with flame-like perthite lamellae. Na (sodium) content within the lamellae is higher than elsewhere in crystal. Width of the image is 4 mm.*

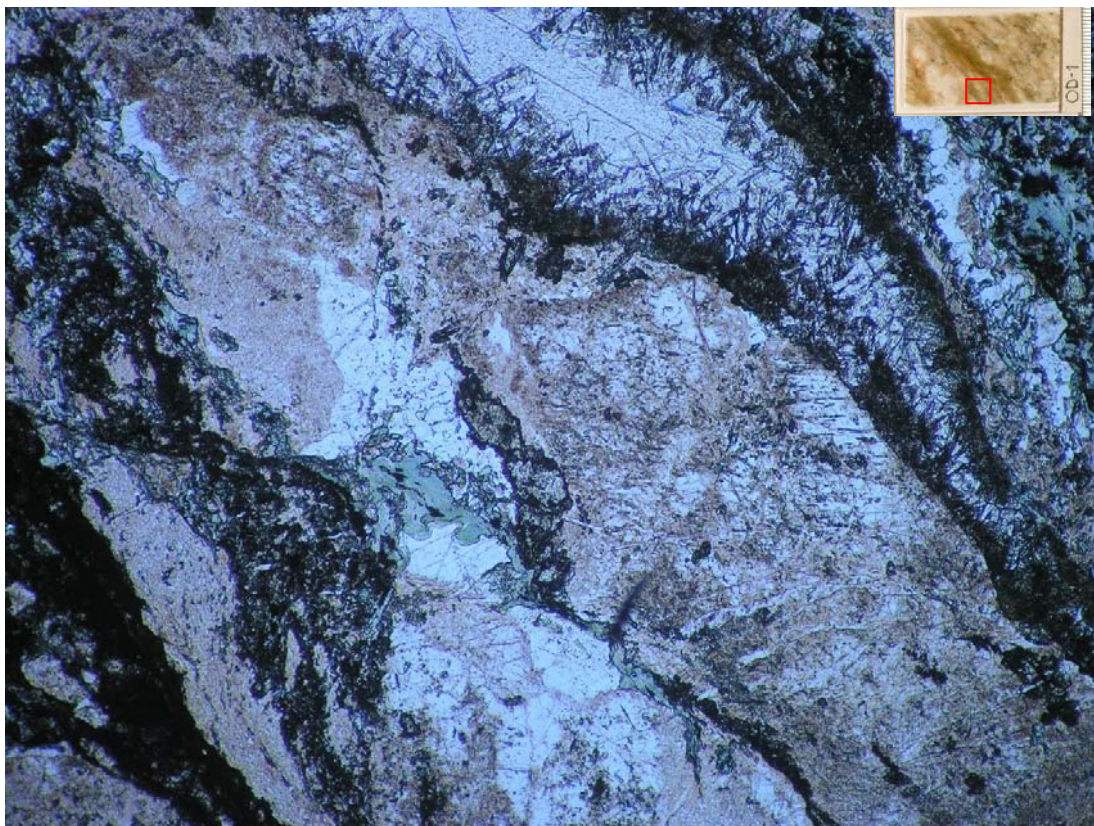


**Microscope image 6:** *Image 5 in non-polarized light. Width of the image is 4 mm.*



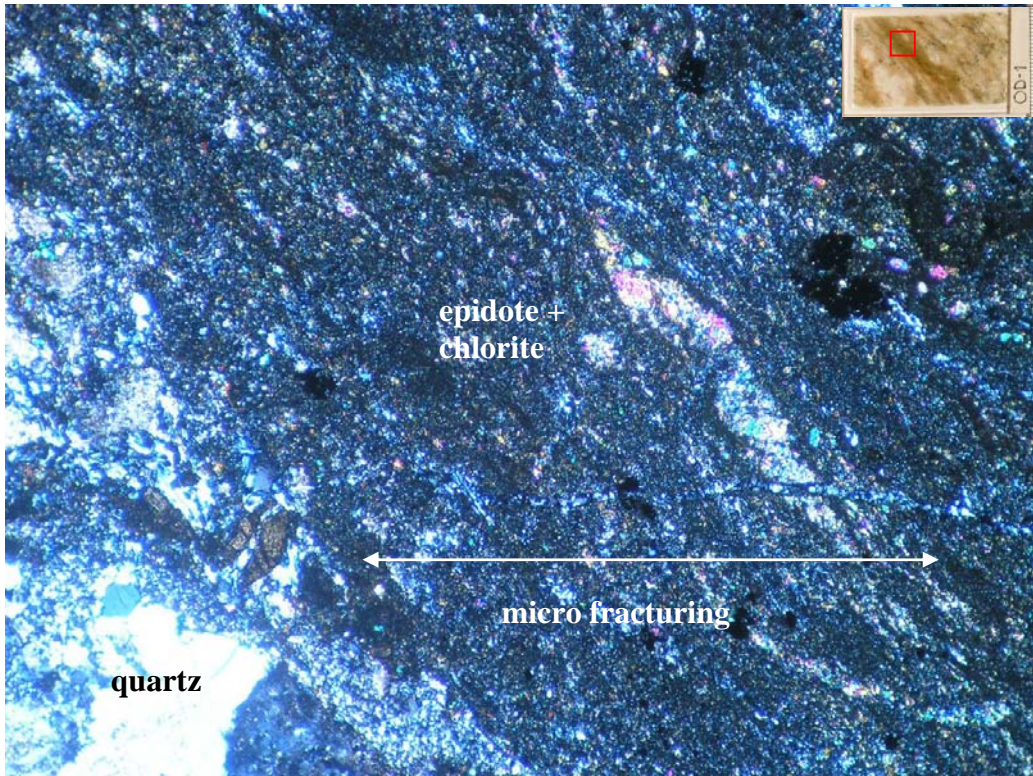


**Microscope image 7:** Oxidized Äspö Diorite 1 (OD-1) in polarized light. Calcite in an epidote vein. Epidote crystals are euhedral, which refers to undisturbed crystallization, probably in an extensional stress environment. Width of the image is 4 mm.

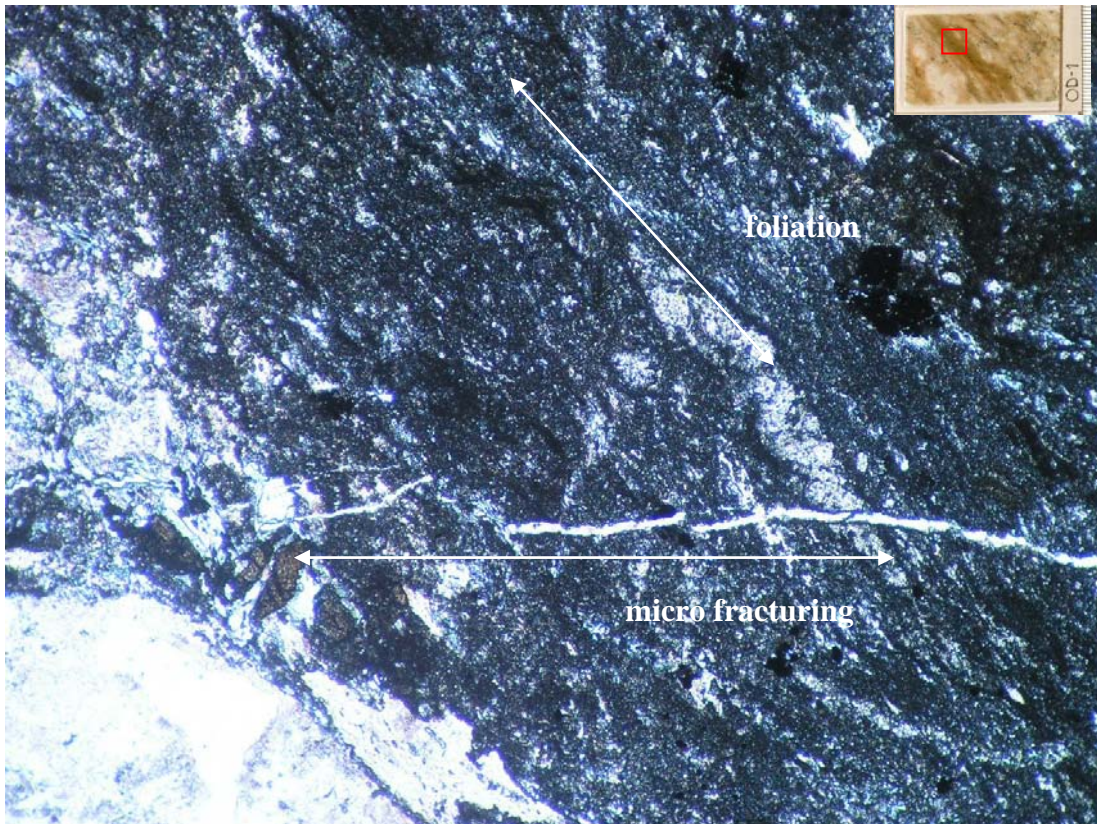


**Microscope image 8:** Image 7 in non-polarized light. Width of the image is 4 mm.



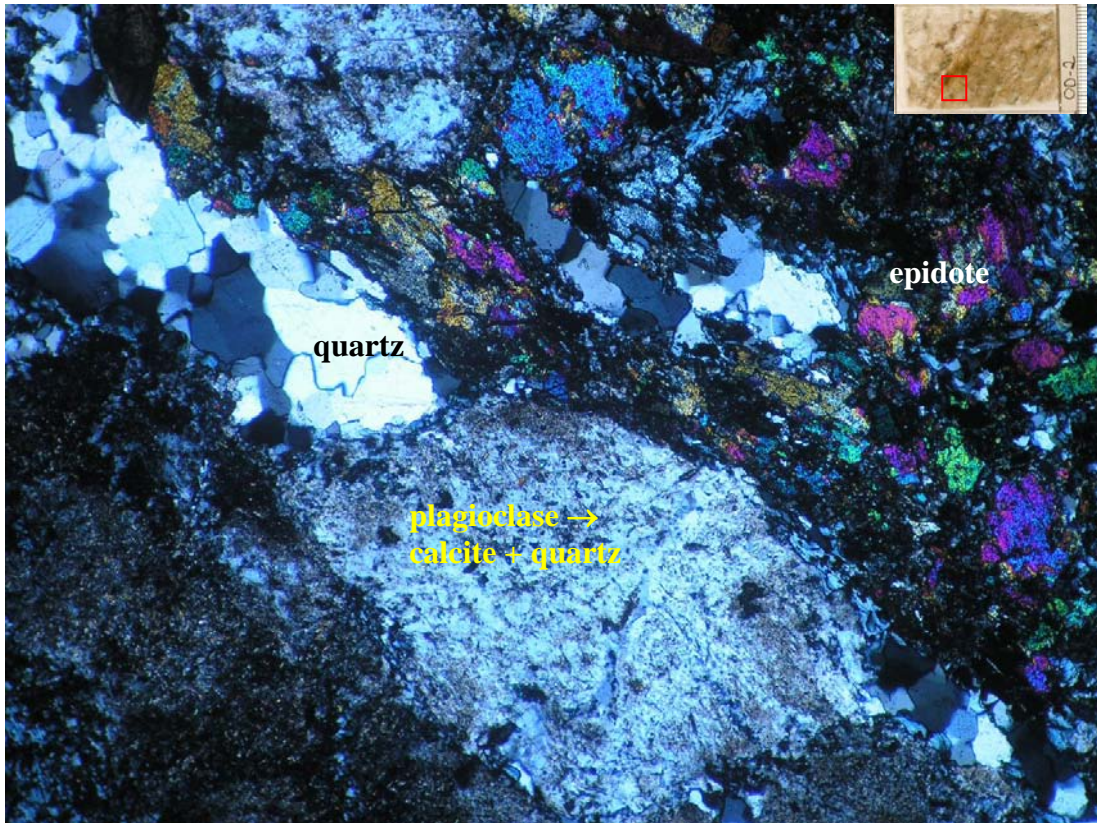


**Microscope image 9:** Oxidized Äspö Diorite 1 (OD-1) in polarized light. Microfracturing in the epidote + chlorite vein (pink and light blue colors) with the *a* geometry anticipated for the spalling-related fracturing. Width of the image is 4 mm.

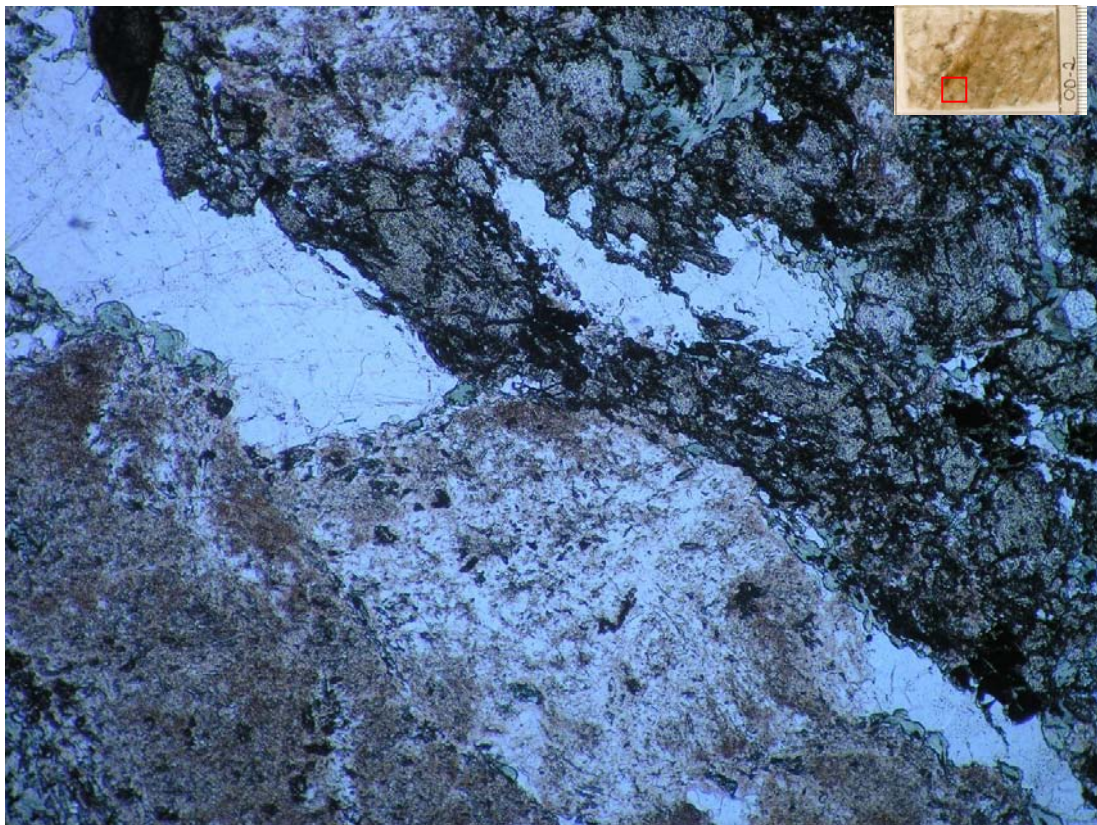


**Microscope image 10:** Image 9 in non-polarized light. The fracturing is here more visible. Width of the image is 4 mm.



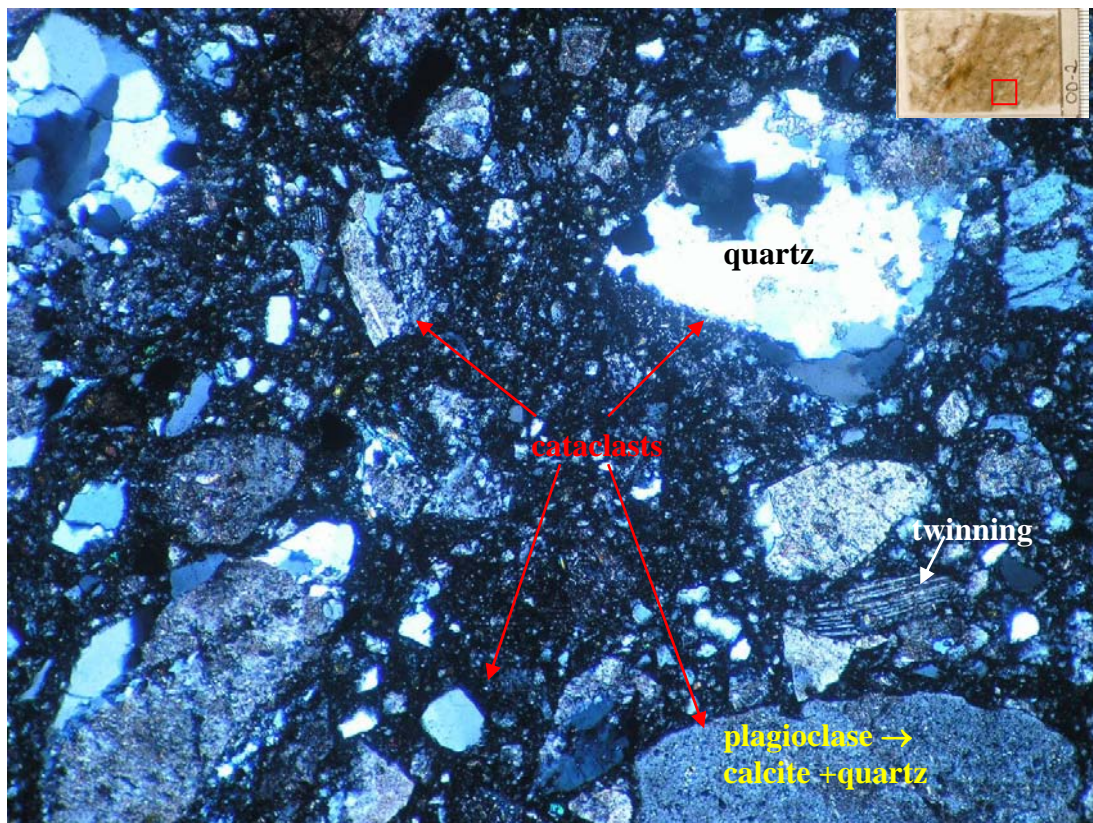


*Microscope image 11: Oxidized Äspö Diorite 2 (OD-2) in polarized light. Altered plagioclase crystals and quartz porphyroclasts. Width of the image is 4 mm.*

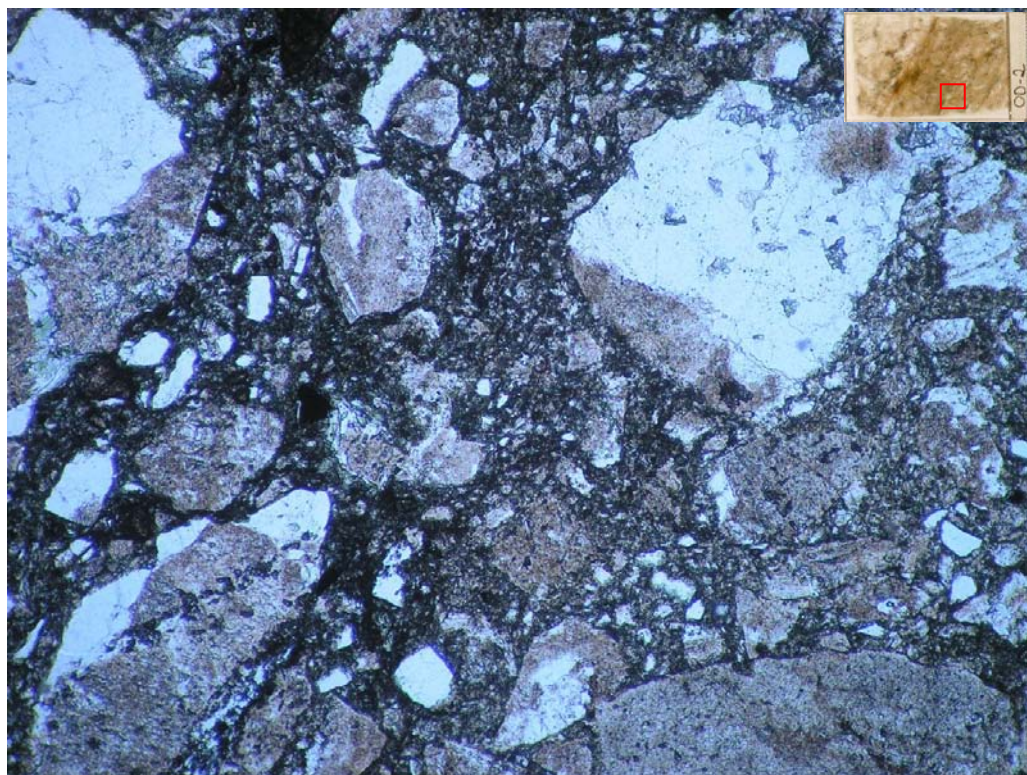


*Microscope image 12: Image 11 in non-polarized light. Width of the image is 4 mm.*



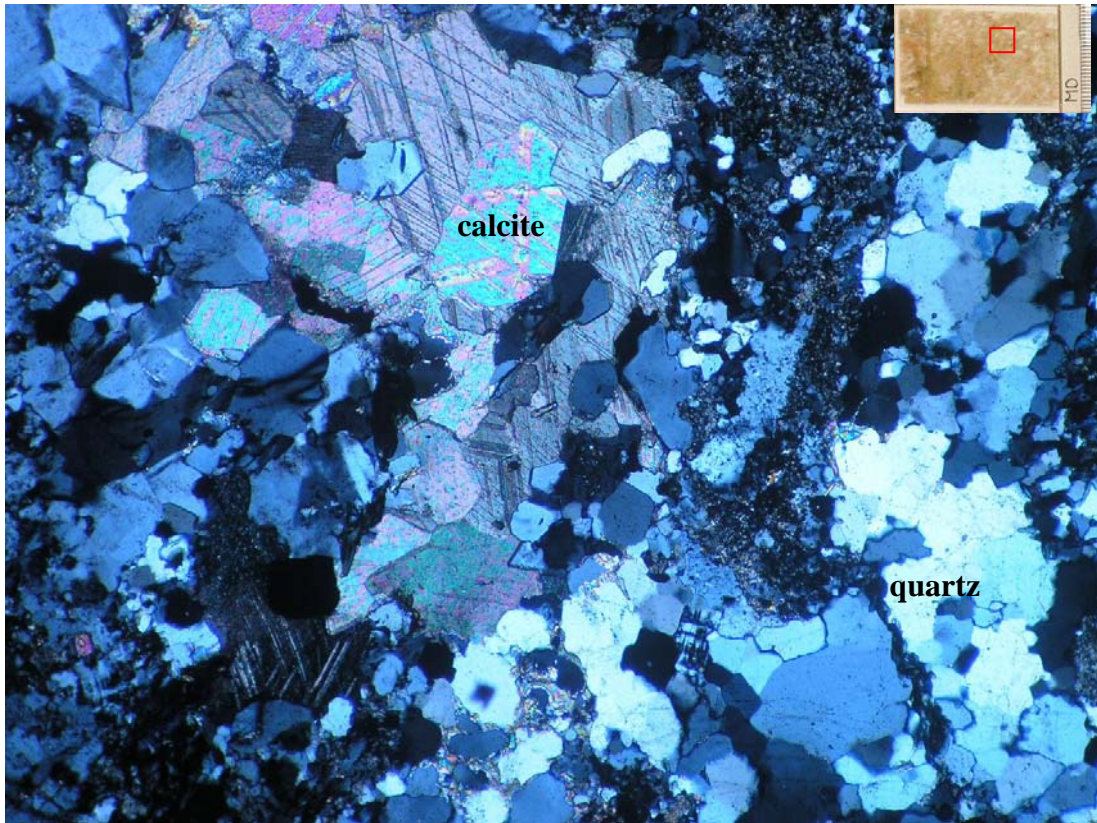


**Microscope image 13:** Oxidized Äspö Diorite 2 (OD-2) in polarized light. Cataclastic shearband with brecciated matrix and sharp porphyroclasts. Some twinning in the altered plagioclase grains. Width of the image is 5 mm.

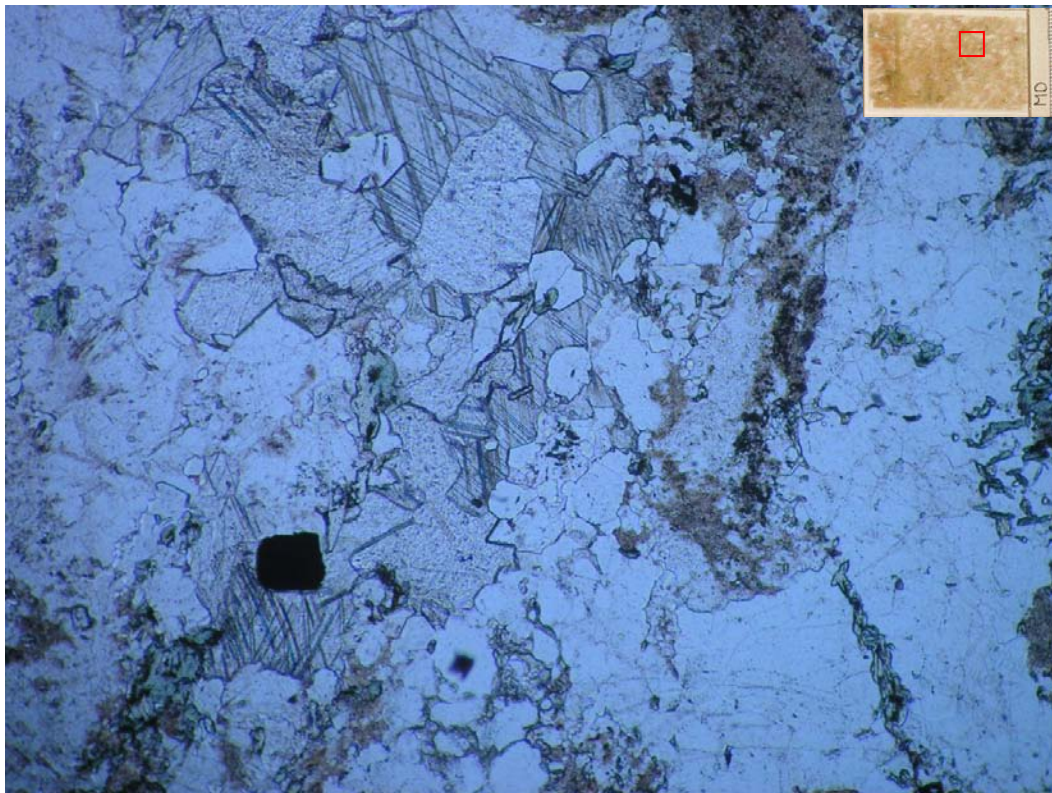


**Microscope image 14:** Image 13 in non-polarized light. Reddish brown hue, caused by the oxidation, is clearly visible. Width of the image is 4 mm.



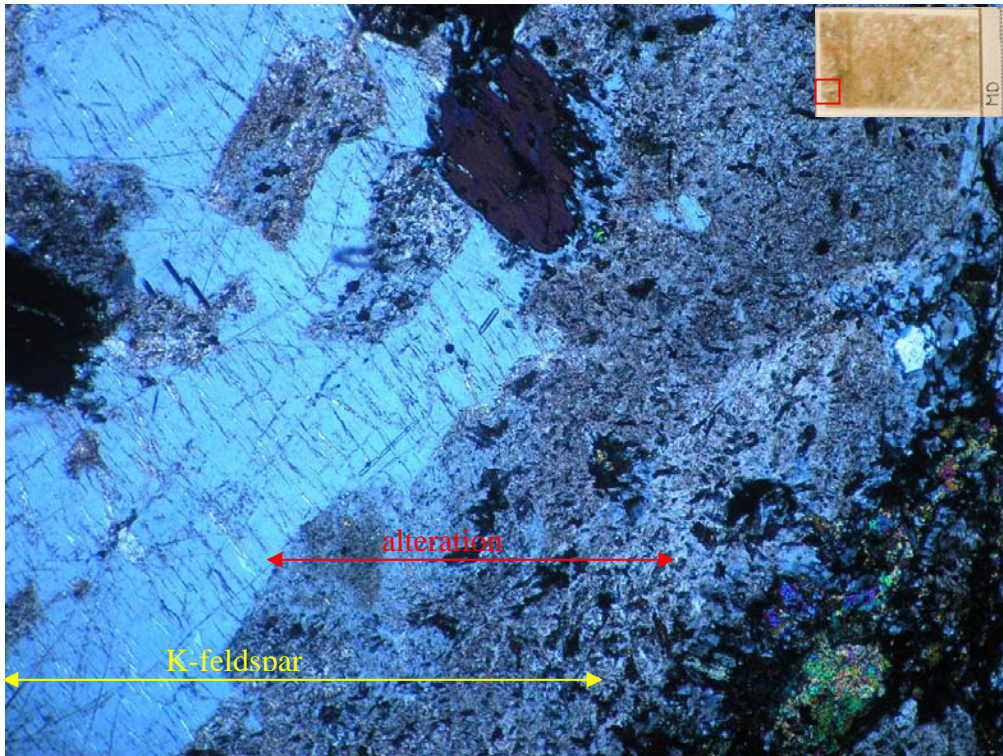


**Microscope image 15:** Mylonitic Äspö Diorite (MD) in polarized light. Thick calcite blebs and veins that have typical calcite crystal twinning. Width of the image is 4 mm.

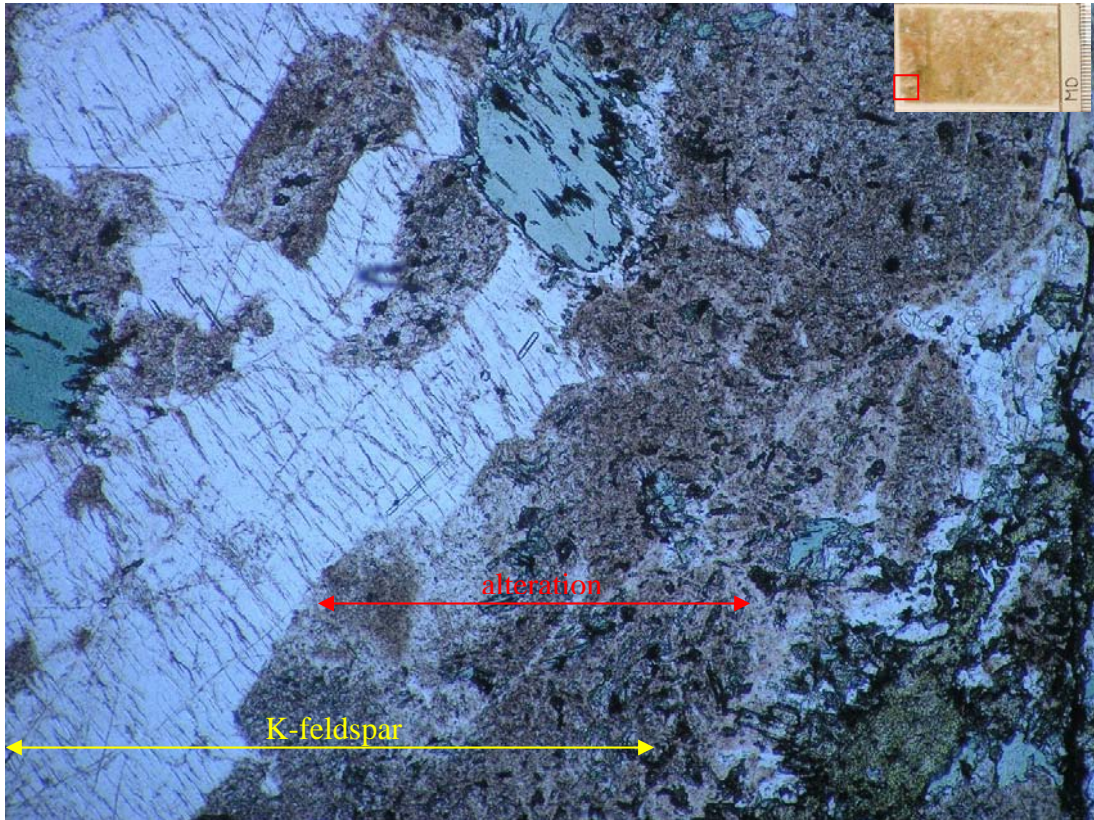


**Microscope image 16:** Image 15 in non-polarized light. Bright green epidote grains are visible. Width of the image is 4 mm.



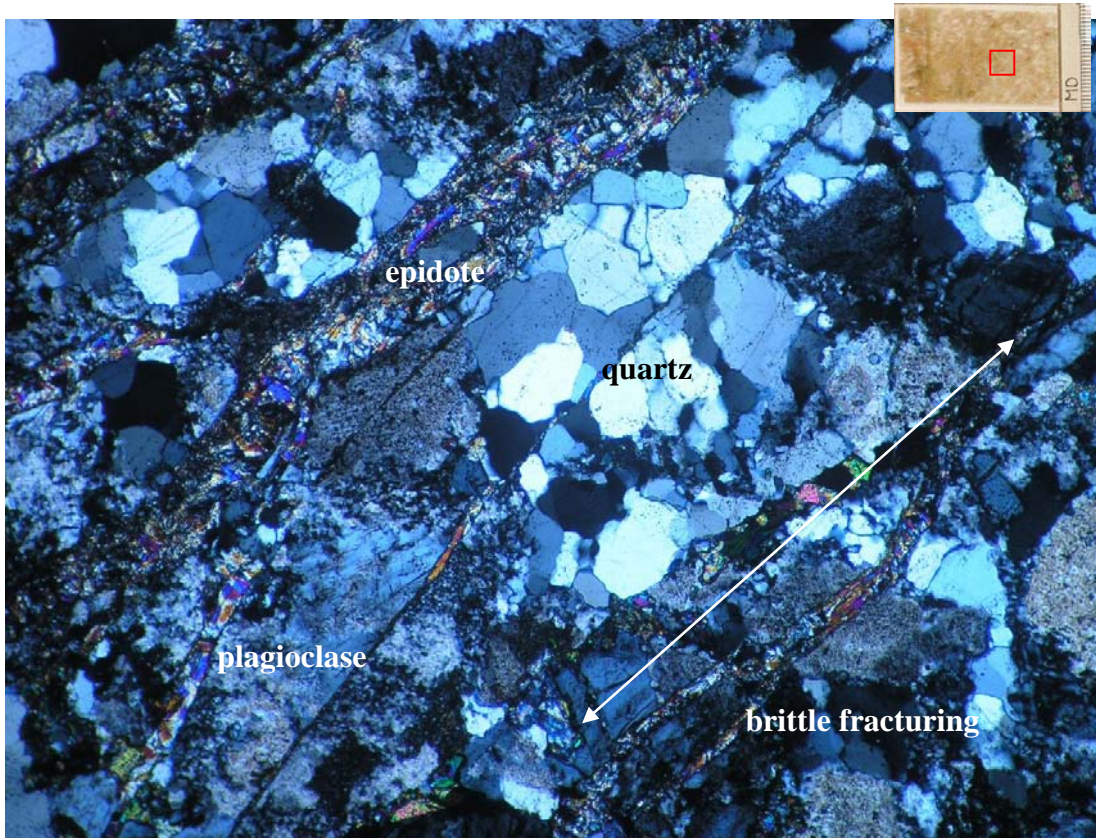


**Microscope image 17:** Mylonitic Äspö Diorite (MD) in polarized light. K-feldspar grain alteration proceeds along a front that moves inward from grain boundaries and fracture and cleavage surfaces. Width of the image is 4 mm.

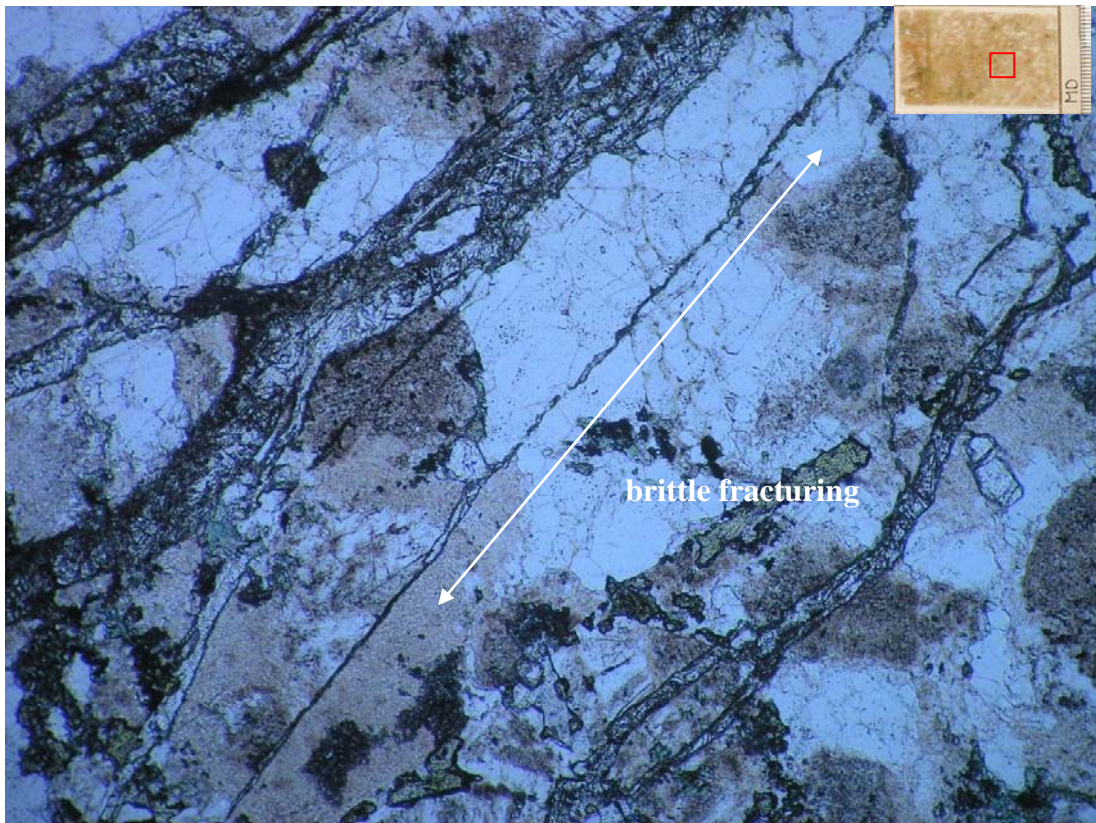


**Microscope image 18:** Image 17 in non-polarized light. Width of the image is 4 mm.



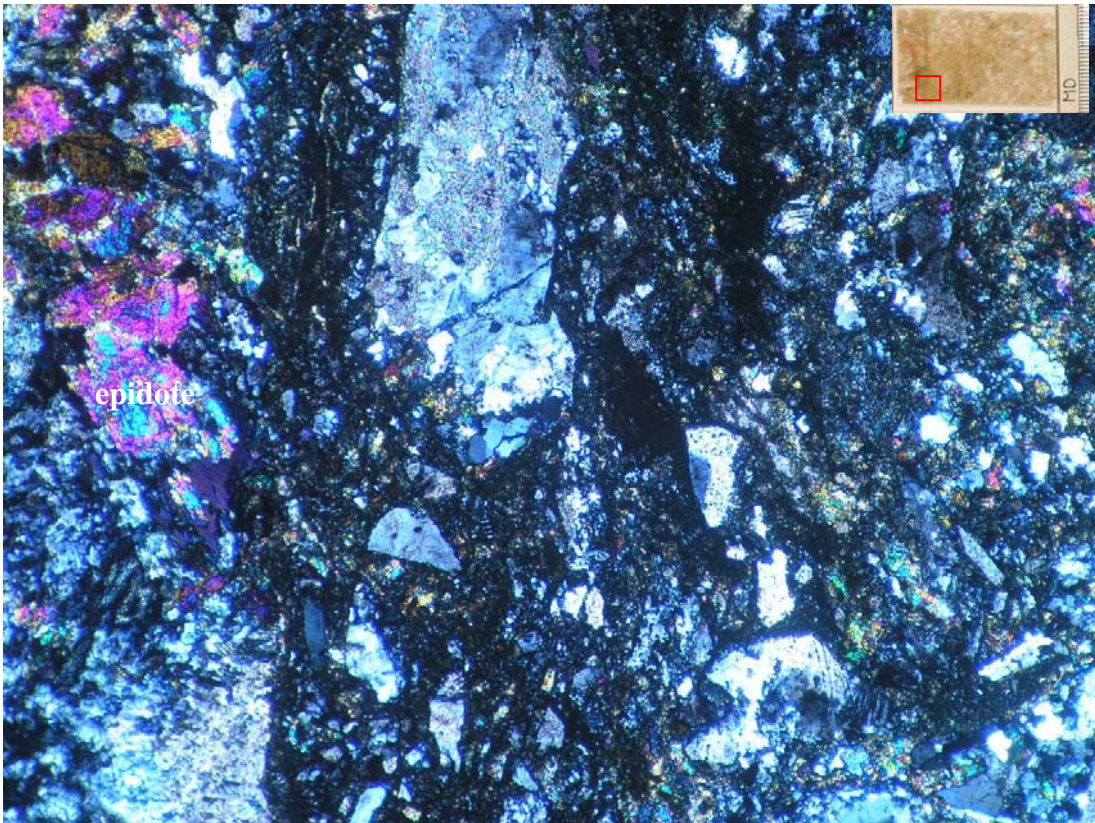


**Microscope image 19:** Mylonitic Äspö Diorite (MD) in polarized light. Altered feldspars, quartz and intense brittle fracturing filled with epidote. Width of the image is 4 mm.



**Microscope image 20:** Image 19 in non-polarized light. Width of the image is 4 mm.





**Microscope image 21:** Mylonitic Äspö Diorite (MD) in polarized light. Epidote vein, which is actually a microscopic cataclastic shear zone. Width of the image is 4 mm.



**Microscope image 22:** Image 21 in non-polarized light. Width of the image is 4 mm.

## APPENDIX 3

### **Geological mapping of the deposition holes DQ0063G01 and DQ0066G01, the slot walls and bottom AQ0064A01, AQ0064B01 and AQ0064G01 and the blocks VQ0061G01 – G05**

#### Mapping

The mapping of the two deposition holes DQ0063G01 and DQ0066G01 was performed by B. Magnor (SKB) and C. Hardenby (SwedPower AB) in the years of 2003-2004. In 2005 C. Hardenby mapped the slot walls, the bottom and the blocks that were the result of the removal of the pillar between the two deposition holes. A. Bäckström (BBK) and D. M. Ivars (Itasca) assisted in part of the slot wall mapping. All the mapping was performed in accordance with the mapping system TMS (Tunnel Mapping System) used by SKB. The maps that were hand drawn underground have been digitized and the associated geological data have been fed into the TMS Access database.

The cut off for fractures was normally 0.5 m. The only exception was the upper parts (about 1 m) of the slot walls where the cut off was about 0.1 m.

The Apse-blocks were moved from their original position in the Q-tunnel at Äspö HRL before the geological mapping took place. Besides the uppermost block, that was not mapped at all, it was only the top surface of each block that was mapped and had new geological data added. Orientations of geological features such as fractures, contacts and deformation zones were originally referred to as angles between the block edges of the top surface and the sides. They were later re-calculated into degrees with reference to magnetic north. The mapping of the block sides facing the slot walls was accomplished by copying appropriate sections from the slot wall mapping and then pasting them on the block sides. Thus, the geological data linked to the block sides is the same as that of the slot walls.



## Legend for geological features

### 1. DQ0063G01

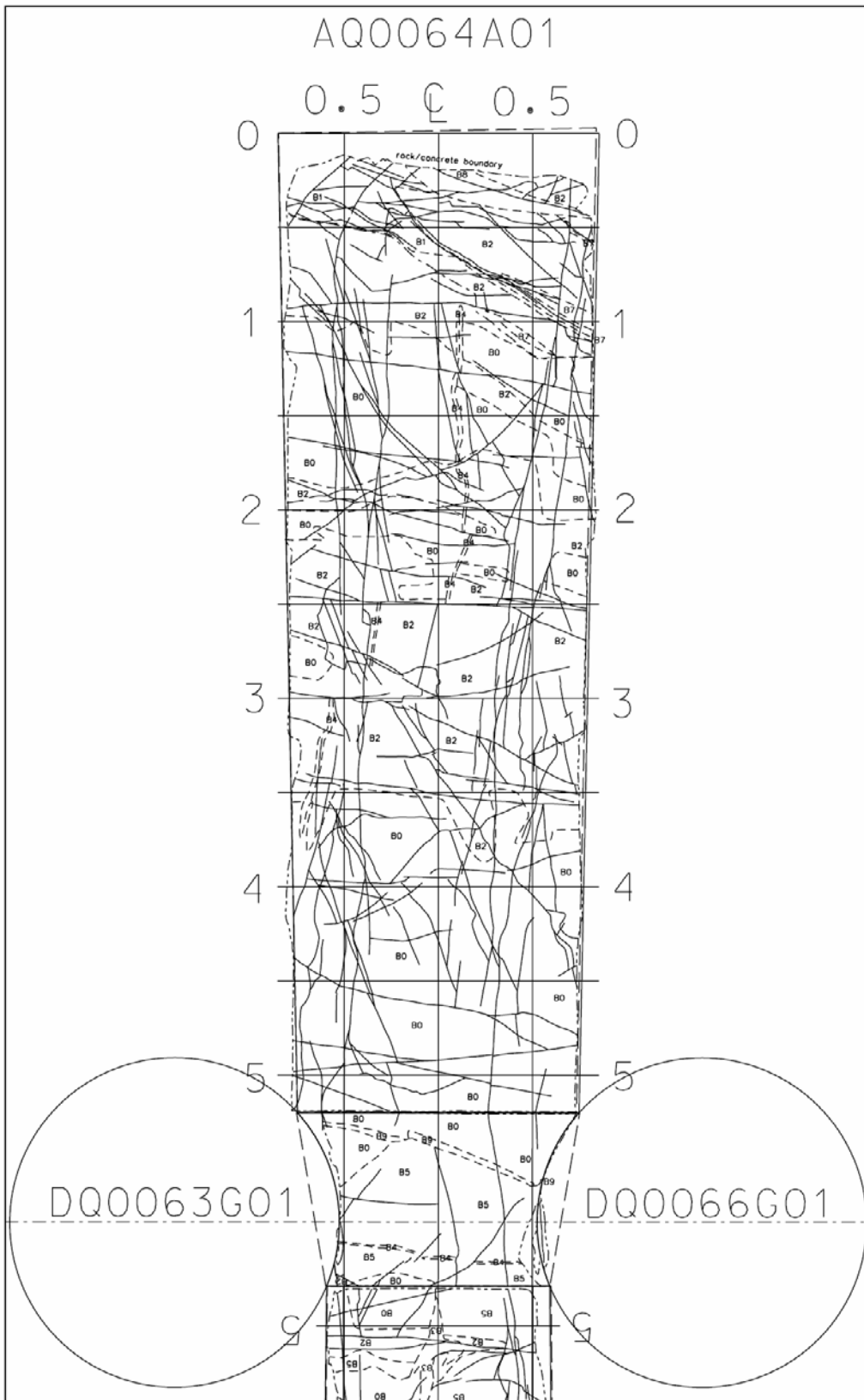
<b>Feature</b>	<b>TMS/map code and/or symbol</b>	<b>Description</b>
Rock types	B1	<u>Äspö diorite</u> , medium grained, reddish grey with feldspar mega-crysts, partly slightly oxidized
	B2	<u>Fine grained granite</u> , reddish
	B3	<u>Pegmatite</u> , medium-coarse grained, reddish
	B4	<u>Äspö diorite</u> , greyish red, mostly oxidized
	B5	<u>Mylonite</u> , greyish red, protomylonitic
	B6	<u>Pegmatite</u> , not a true pegmatite, more like granitization, medium grained, reddish
Contacts	K0-K4, with dashed line	
Fractures	Continuous line	
Deformation zones	Z0, with dash-dot line	
Water	A-H	
	v=damp, single drops	
	vv=seepage, drops	
	vvv=flow	

2. DQ0066G01

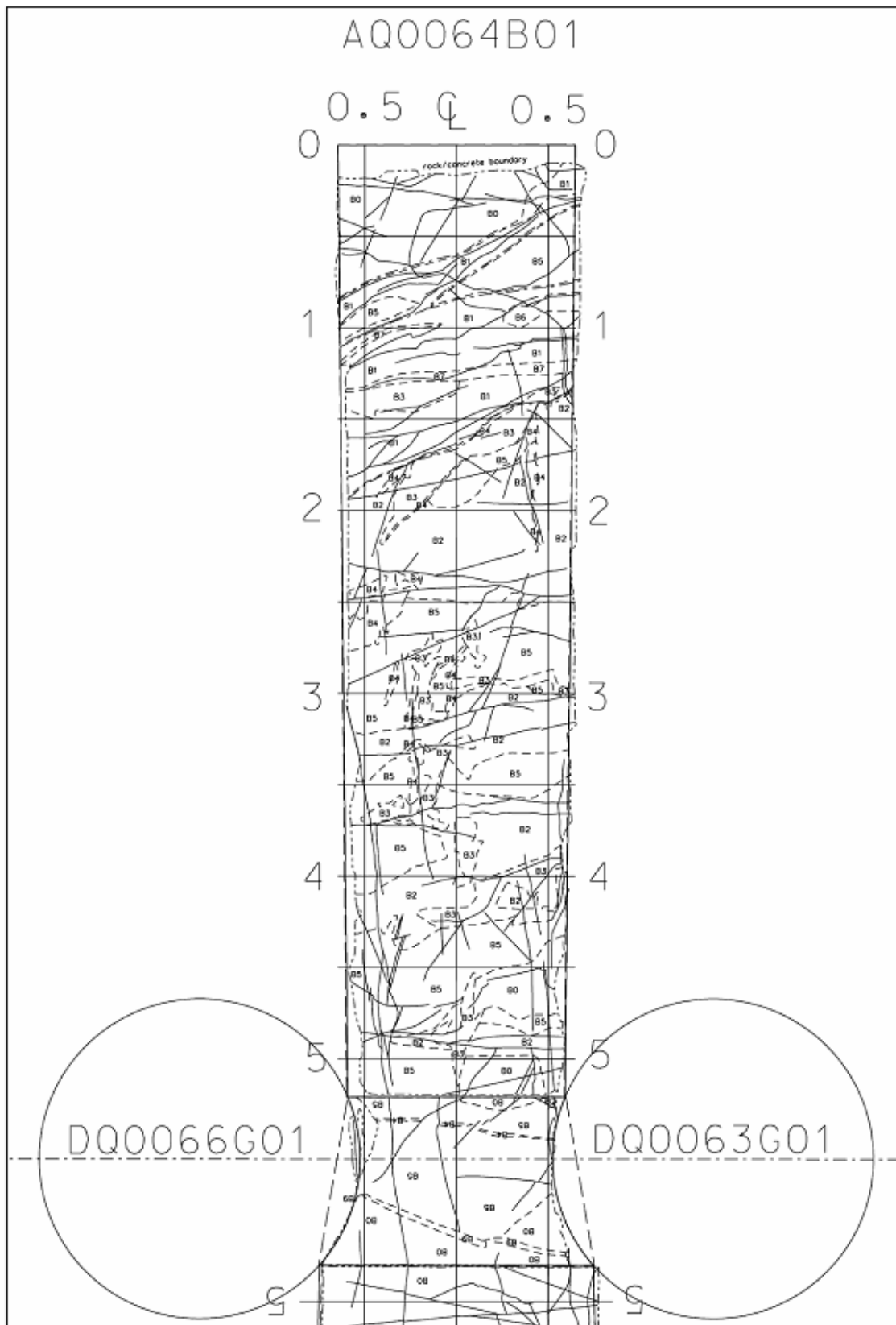
<b>Feature</b>	<b>TMS/map code and/or symbol</b>	<b>Description</b>
Rock types	B1	Äspö diorite, medium grained, reddish grey with feldspar mega-crysts
	B2	<u>Pegmatite</u> , medium-coarse grained, reddish, irregular texture
	B3	<u>Fine grained granite</u> , fine-medium grained, reddish, homogeneous texture
	B4	<u>Äspö diorite</u> , reddish grey, mostly oxidized
	B5	<u>Mylonite</u> , sheared zone not entirely mylonitic, fine grained, greyish red
Contacts	K0-K6, with dashed line	
Fractures	Continuous line	
Deformation zones	Z0-Z1, with dash-dot line	
Water	A-I	
	v=damp, single drops	
	vv=seepage, drops	
	vvv=flow	

### 3. Slot walls, bottom and blocks

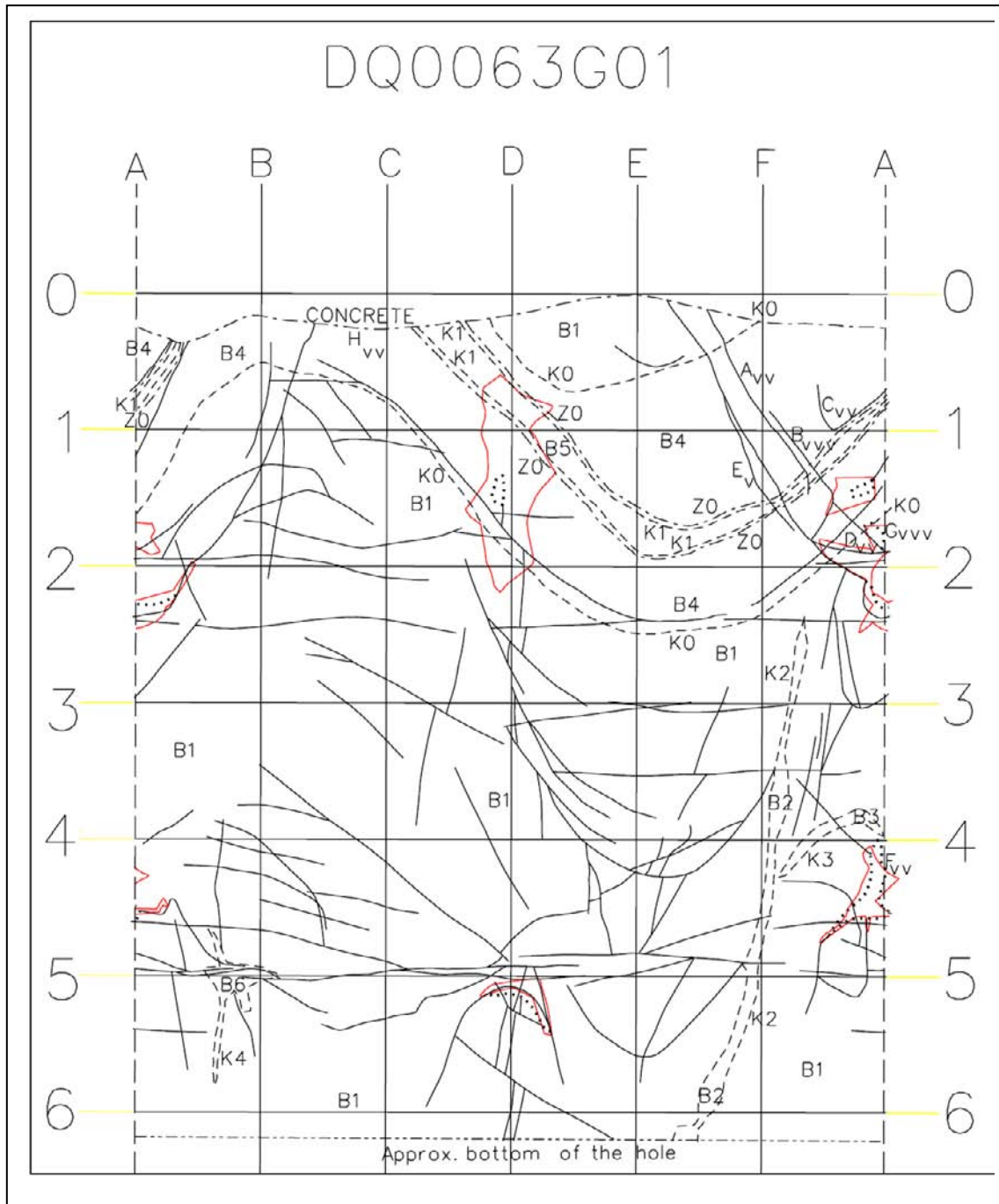
Feature	TMS/map code and/or symbol	Description
Rock types	<p>B0</p> <p>B1</p> <p>B2</p> <p>B3</p> <p>B4</p> <p>B5</p> <p>B6</p> <p>B7</p> <p>B8</p> <p>B9</p> <p>B10</p>	<p><u>Äspö diorite</u>, medium grained, grey with pinkish feldspar mega-crysts</p> <p><u>Äspö diorite</u>, medium grained, greyish red-red, often irregular texture, epidote healed fracture pattern, partly brecciated</p> <p><u>Äspö diorite, oxidized</u>, medium grained with feldspar mega-crysts, greyish red, minor epidote healed fractures, partly somewhat brecciated</p> <p><u>“Fine grained” granite, probably a hybrid rock</u>, medium grained, reddish, within deformation zones partly brecciated</p> <p><u>Pegmatite</u>, medium-coarse grained, light red-red</p> <p><u>Äspö diorite</u>, medium grained with feldspar mega-crysts, reddish grey, intermediate between B0-B1 or B0-B2</p> <p><u>Äspö diorite, brecciated</u> with epidote matrix, medium grained, irregular texture, greenish-reddish</p> <p><u>Mylonite</u>, fine grained, reddish grey-yellowish grey, more or less mylonitic, schistified-sheared</p> <p><u>Breccia</u>, medium grained, greenish, irregular texture and structure, epidote matrix</p> <p><u>Quartz vein</u>, fine grained, homogeneous, mostly with oxidation rim outside</p> <p><u>“Fine grained granite”, hybrid rock</u>, fine grained, reddish, fractured-brecciated with epidote matrix</p>
Contacts	Dashed line	
Fractures	Continuous line	Includes both natural and man made fractures
Deformation zones	Dash-dot line	



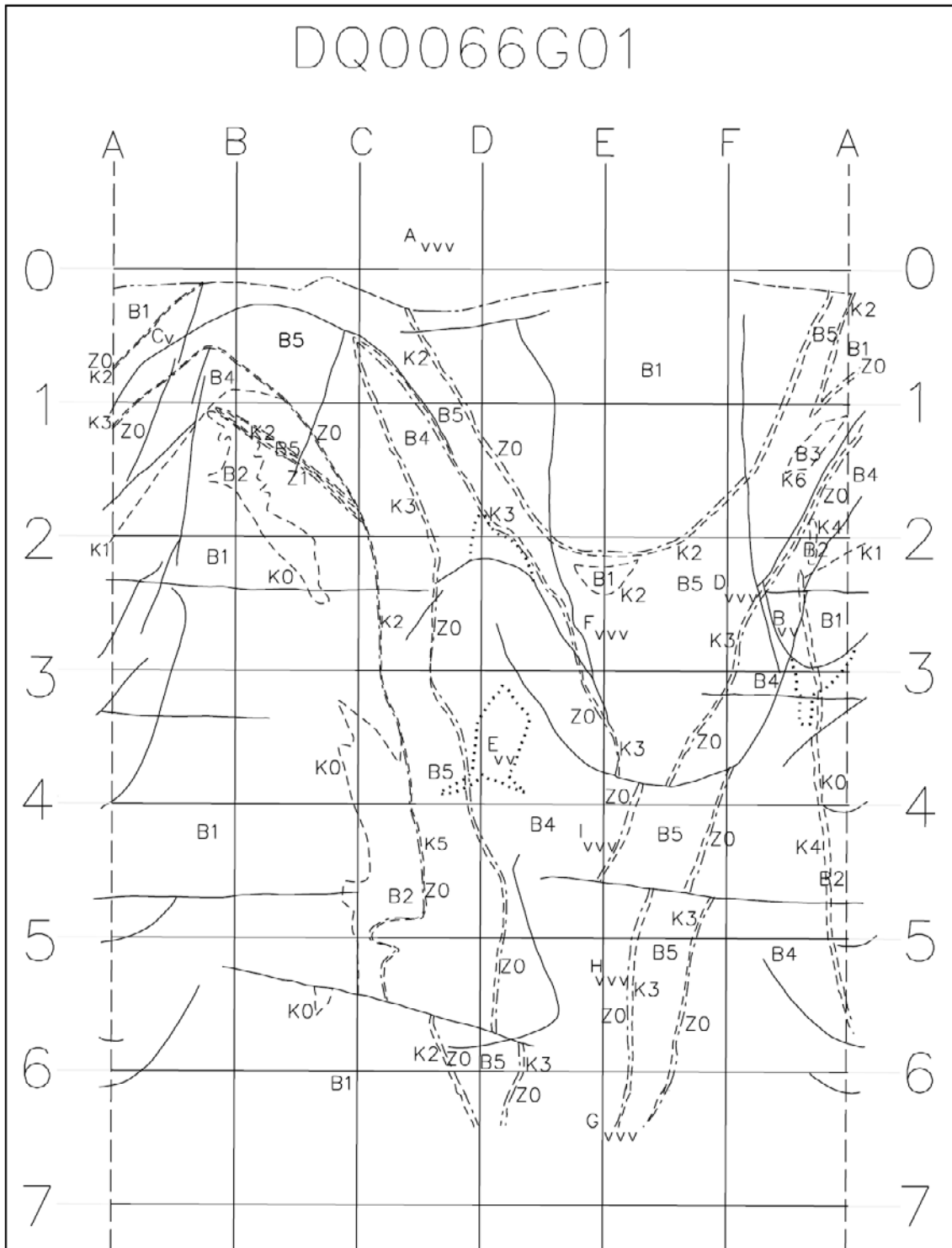
**Figure 1.** The A-wall, the left wall when one is looking towards tunnel front (face).



**Figure 2.** The B-wall, the right wall when one is looking towards tunnel front (face).

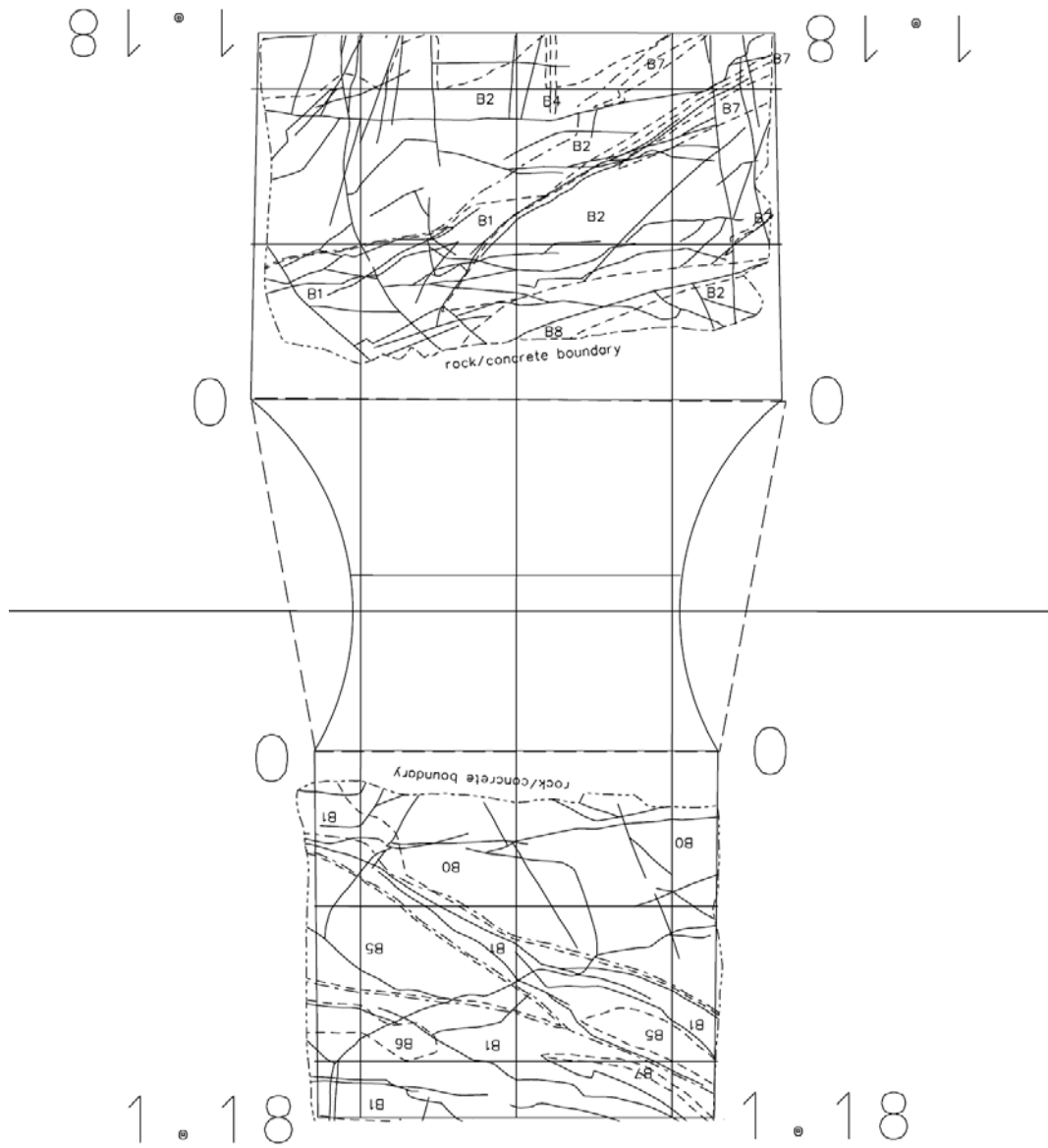


**Figure 3.** The mapping image of the canister hole DQ0063G01, which was open during the APSE experiment. The cylinder representing the canister hole is bent open in this digitation. The numbers in the sides present the vertical depth of a hole. Red lines indicate areas where minor spalling occurred during the excavation of the hole.



**Figure 4.** The mapping image of the canister hole DQ0066G01, which was confined during the APSE experiment. The cylinder representing the canister hole is bent open in this digitation. The numbers in the sides present the vertical depth of a hole.

Left side (A)



Right side (B)

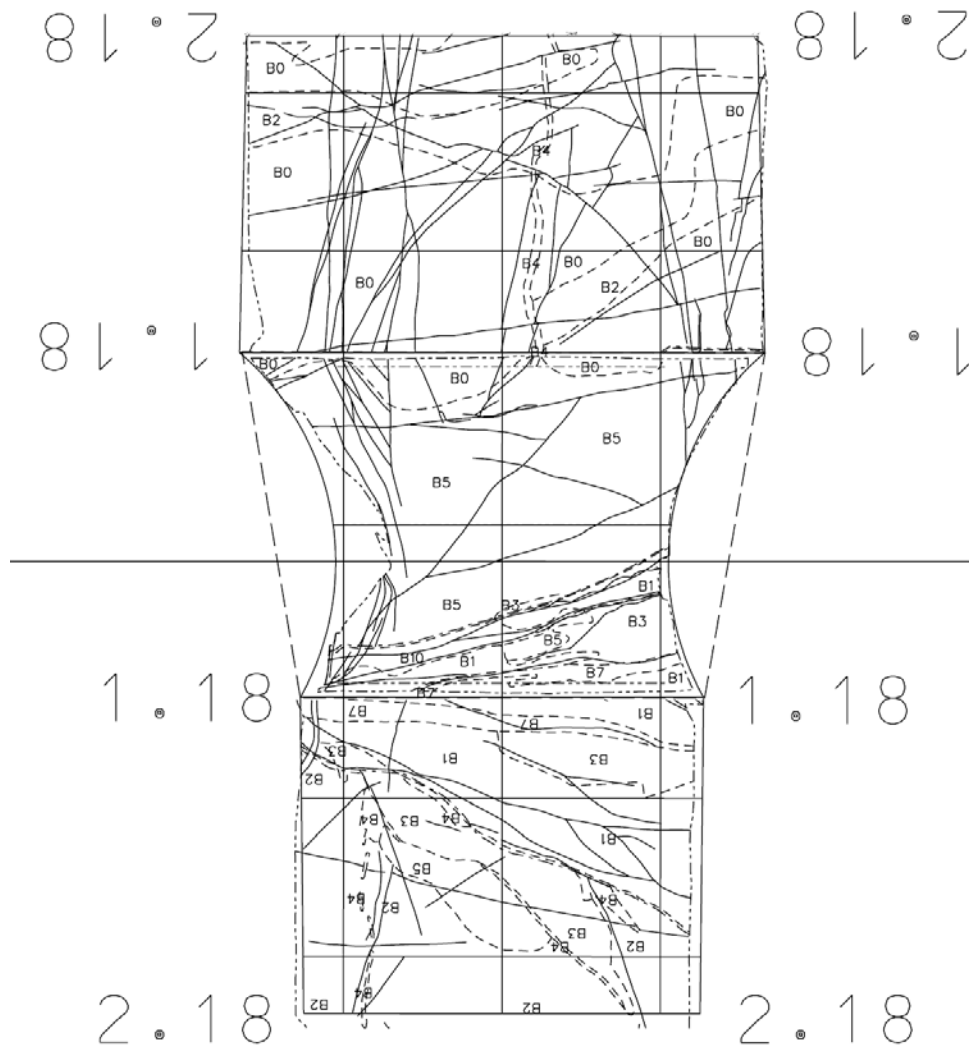
Block no 1 (Top block)

VQ0064G01

*Figure 4. The digitised map image of the APSE block number 1.*



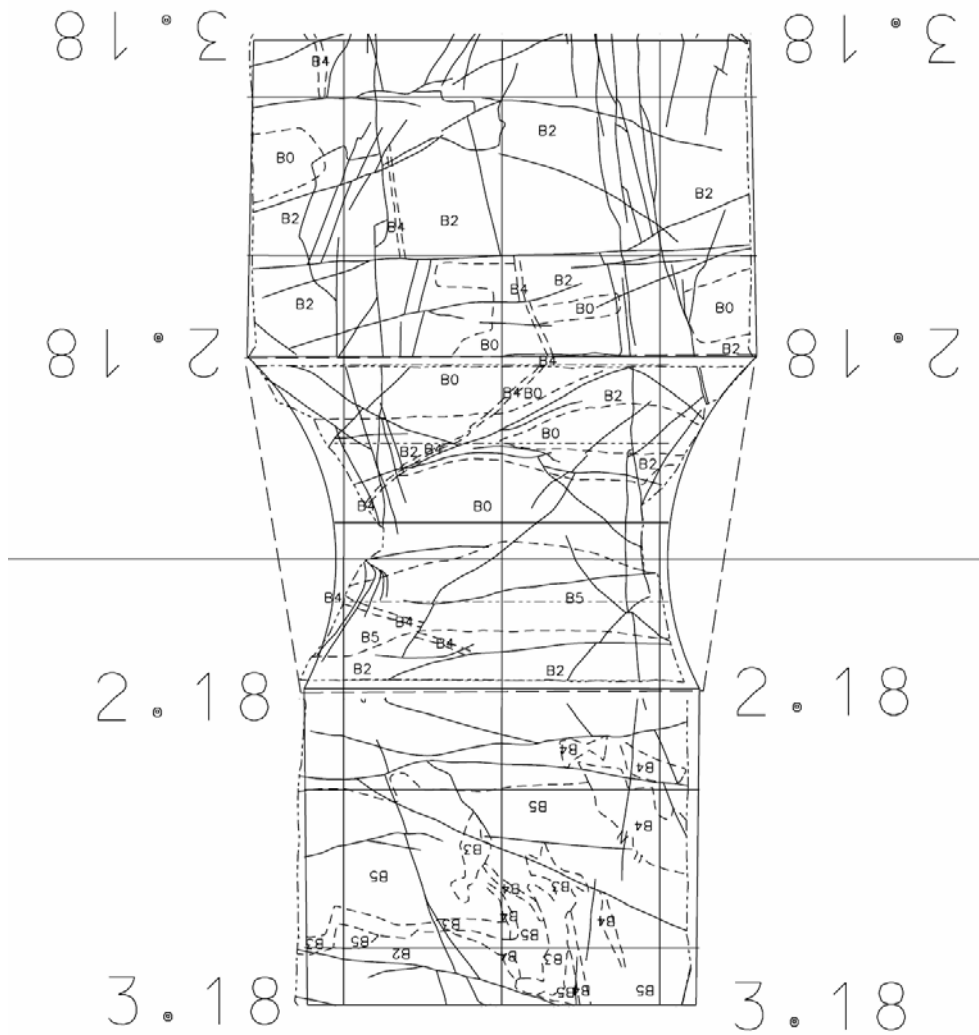
Left side (A)



Right side (B)  
Block no. 2  
VQ0064G02

*Figure 5. The digitised map image of the APSE block number 2.*

Left side (A)



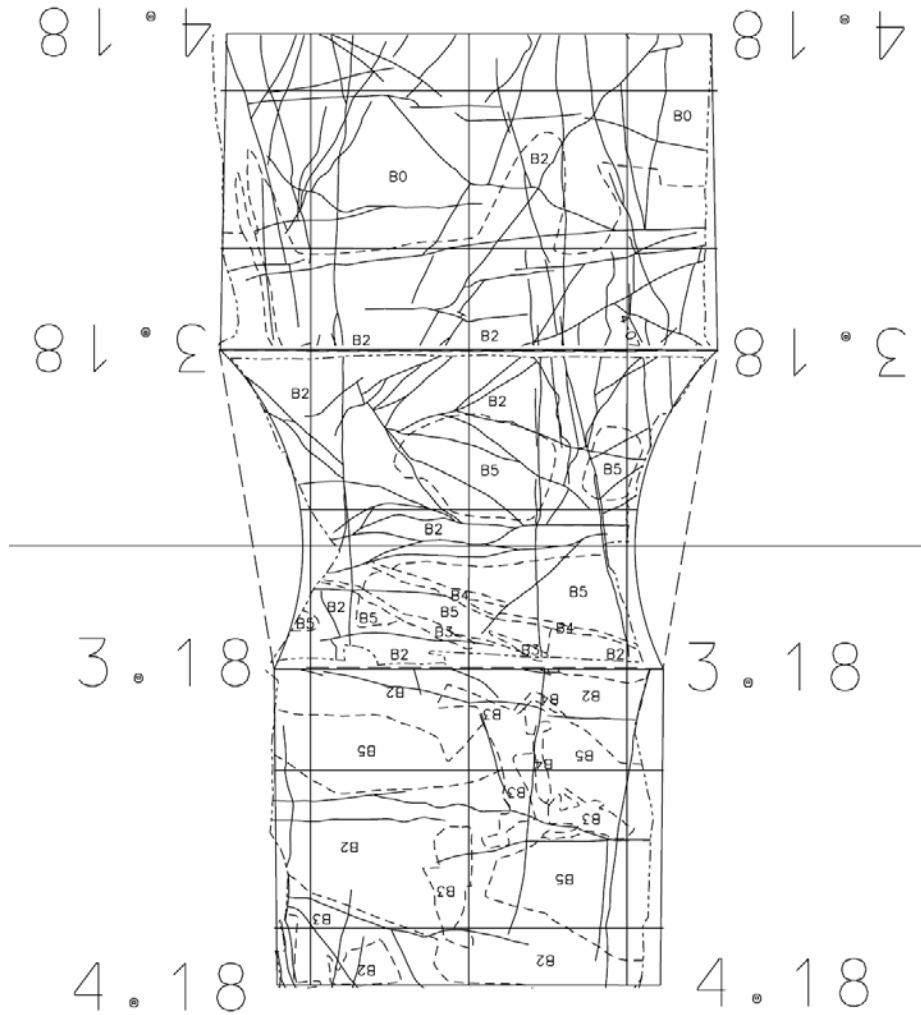
Right side (B)

Block no. 3

VQ0064G03

*Figure 6. The digitised map image of the APSE block number 3.*

Left side (A)



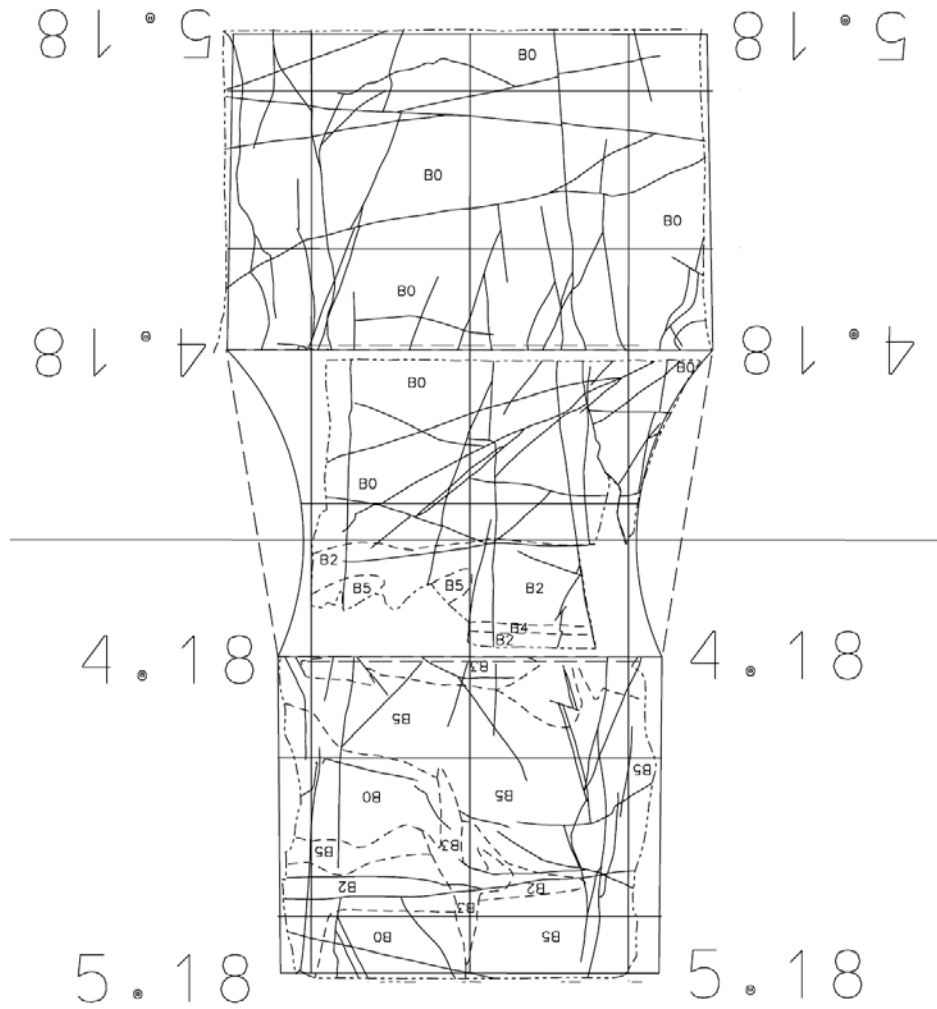
Right side (B)

Block no. 4

VQ0064G04

*Figure 7. The digitised map image of the APSE block number 4.*

Left side (A)

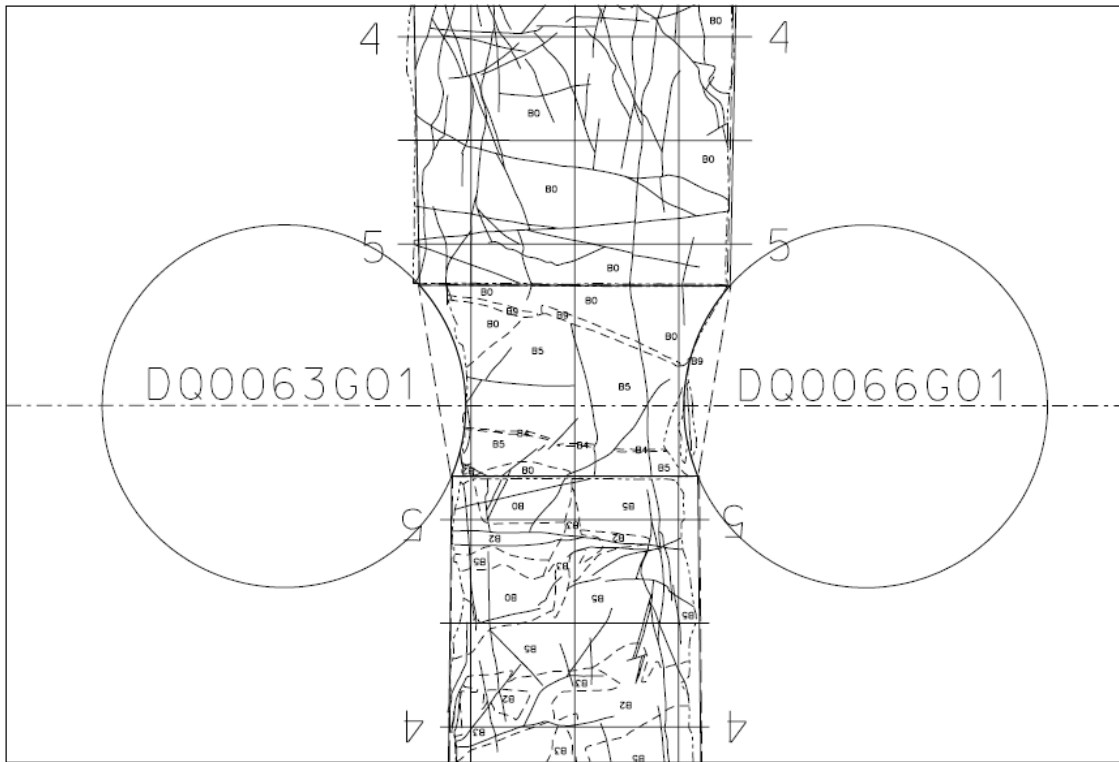


Right side (B)

Block no. 5

VQ0064G05

**Figure 8.** The digitised map image of the APSE block number 5.



*Figure 9. The bottom side of the APSE block number 5.*

